Chapter 10

Hits and Lead Discovery in the Identification of New Drugs against the Trypanosomatidic Infections

Theodora Calogeropoulou,[1,*] *George E. Magoulas,*[1] *Ina Pöhner,*[2] *Rebecca C. Wade,*[2,8,9] *Joanna Panecka-Hofman,*[2,3,9] *Pasquale Linciano,*[4] *Stefania Ferrari,*[4] *Maria Paola Costi,*[4,*] *Nuno Santarem,*[5] *M[a] Dolores Jiménez-Antón,*[5] *Ana Isabel Olías-Molero,*[5] *Anabela Cordeiro da Silva*[5,7] and *José María Alunda*[6]

INTRODUCTION

The Neglected Tropical Diseases (NTDs) are a group of 17 pathologies, recognized by the World Health Organization (WHO), which are endemic in 149 countries of tropical and sub-tropical areas of the globe, and affect more than one billion people overall (Feasey et al. 2010). The pathologies are all caused by microparasites or macroparasites. Among the diseases provoked by microparasites, three are caused by kinetoplastidae, a group of flagellated protozoa transmitted by insect vectors: Chagas disease, Human African Trypanosomiasis and leishmaniasis. The focus of the present chapter is on the identification of new drugs for the treatment of trypanosomatidic infections such as Chagas disease, caused by *Trypanosoma cruzi,* and Human African Trypanosomiasis, caused by *Trypanosoma brucei* (Filardy et al. 2018).

[1] Institute of Biology, Medicinal Chemistry and Biotechnology, National Hellenic Research Foundation, Athens, Greece.
[2] Molecular and Cellular Modeling Group, Heidelberg Institute for Theoretical Studies (HITS), Heidelberg, Germany.
[3] Faculty of Physics, University of Warsaw, Warsaw, Poland.
[4] University of Modena and Reggio Emilia, Via Campi 103, 41125 Modena, Italy.
[5] Instituto de Investigação e Inovação em Saúde, Universidade do Porto, and Parasite Disease Group, Instituto de Biologia Molecular e Celular, Universidade do Porto, Porto, Portugal.
[6] Department of Animal Health, Faculty of Veterinary Medicine, Universidad Complutense de Madrid, Madrid, Spain.
[7] Departamento de Ciências Biológicas, Faculdade de Farmácia da Universidade do Porto, Porto, Portugal.
[8] Center for Molecular Biology (ZMBH), DKFZ-ZMBH Alliance, Heidelberg University, Heidelberg, Germany.
[9] Interdisciplinary Center for Scientific Computing (IWR), Heidelberg University, Heidelberg, Germany.
* Corresponding authors: tcalog@eie.gr; costimp@unimore.it

Au.: PI check

Chagas Disease

Chagas disease, also referred to as American Trypanosomiasis, represents a serious medical and socioeconomic burden for over 21 regions of Latin America. More than 8 million people worldwide are estimated to be infected by *T. cruzi* and more than 10,000 deaths per year are reported. Recently, a reduction in incidence and prevalence of the infection has been observed, but on the other hand, a spread of the disease to previously unaffected regions as a consequence of massive migration fluxes, congenital transmission, and blood and organ donations has been reported, making Chagas disease a world health issue (Figure 1) (Pérez-Molina and Molina 2018).

The disease usually evolves from an acute to a chronic phase. The acute phase arises just after the infection and can last from a few weeks to several months and is characterized by non-specific symptoms (i.e., fever, swelling of skin and mucosa). Thereafter, the disease enters an asymptomatic chronic stage and only 20–30% of the infected people manifest lethal complications after several years (Bern et al. 2011). The treatment of both the acute and chronic stages of Chagas disease is based on chemotherapy. For almost 50 years, benznidazol and nifurtimox (Figure 2) were the two first-line drugs for the treatment of Chagas disease (Rodriques Coura and de Castro 2002). Unfortunately, their efficacy is limited, and more frequently the side effects that the two drugs elicit during the treatment of the chronic stage induce the patients to quit the therapy. Nifurtimox treatment is discontinued in up to 75% of all cases, and benznidazol, which is better tolerated, is discontinued in 9 to 29% of the cases. Besides chemotherapy, serological cure is recommended for acute congenital Chagas during the first year of life, and for chronically infected children under 14 years (Pérez-Molina and Molina 2018).

Human African Trypanosomiasis (HAT)

Human African Trypanosomiasis (HAT), also known as sleeping sickness, is caused by the bloodstream form of the two protozoan parasites *Trypanosoma brucei gambiense* and *Trypanosoma brucei rhodesiense* (Büscher et al. 2017). The sleeping sickness is mainly spread in the poorest rural area of sub-Saharan Africa,

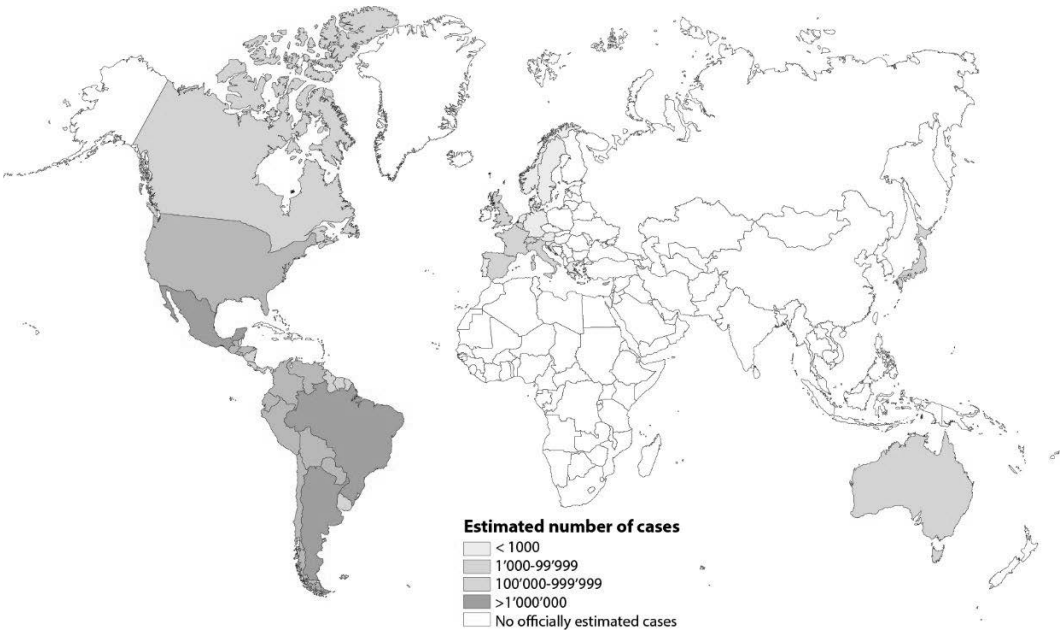

Figure 1. Incidence of *T. cruzi* infection, based on official estimates and status of vector transmission. Adapted from WHO 2010.

Color version at the end of the book

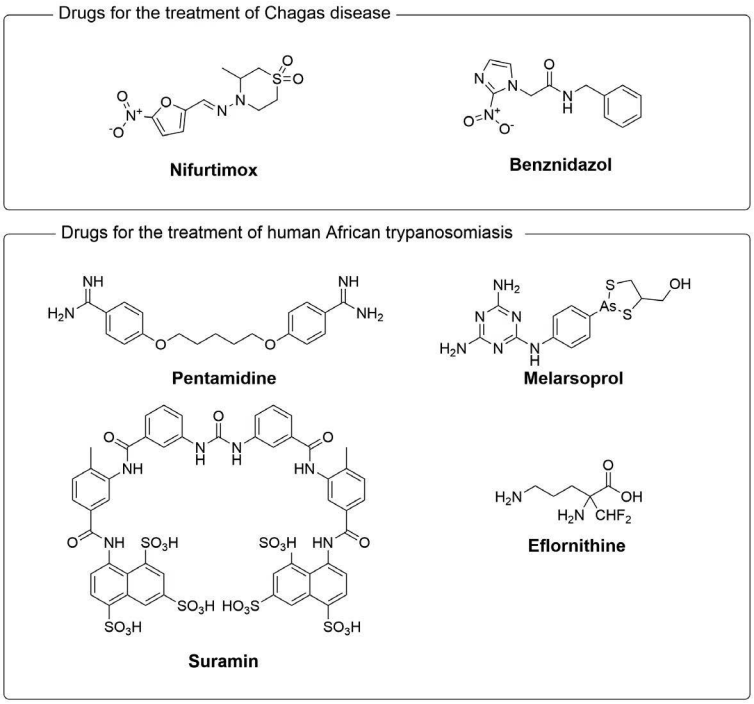

Figure 2. Drugs currently in use for the treatment of Chagas disease and Human African Trypanosomiasis.

where the habitat is suitable for the survival of the tsetse fly, the vector responsible for the transmission of the parasite. In particular, *T. b. gambiense* is widespread in Central and Western Africa and causes over 98% of chronic HAT, whereas *T. b. rhodensiense* only infects humans occasionally and is mainly spread in Southern and Eastern Africa (Figure 3). Starting from 2009, and for the first time in thirty years, mostly due to WHO launched programs of surveillance and treatment, less than 10.000 new cases per year of HAT were registered in 2009. This represents a drop of 76% with respect to the 300,000 cases observed in 1995. This trend suggests that a complete eradication of HAT by 2020 is possible (WHO 2017). However, the number of cases registered by the WHO covers only the visible part of HAT incidence, whereas around 70 million people living in sub-Saharan Africa are exposed to *T. brucei* infection (Simarro et al. 2012).

HAT can occur in an acute or chronic form. The acute form of the disease appears within few weeks of the initial injection of the trypomastigote form of the parasite into the host by the tsetse fly. It is characterized by non-specific flu-like symptoms including fever, headache and joint pain. Thereafter, similar to Chagas disease, the infection can remain quiescent for a long time period and re-emerge several years later (chronic form). The second stage starts when the parasite migrates across the blood-brain barrier into the central nervous system, resulting in neurological symptoms such as confusion, depleted coordination, sensory disturbances and disruption of the normal sleeping cycle (from which the name sleeping sickness was derived). Ultimately, progressive mental deterioration leads to coma and death (Kennedy 2013). Beside *T. b. gambiense* and *rhodesiense*, pathogens for humans, other *Trypanosoma species* (e.g., *T. vivax*, *T. congolense* and *T. brucei evansi*) are etiological agents of a variety of wasting diseases affecting domestic livestock, which collectively go by the name of Animal African Trypanosomiasis (AAT or Nagana). Nagana causes significant damage to cattle farming with 3 million heads lost each year, contributing to significant economical damage in countries with already fragile economic structures. Moreover, animals represent a reservoir for these parasites from which humans may be exposed to infection (Njiokou et al. 2010). Therefore, fighting both HAT and AAT in the one health approach (Okello et al. 2014) is the only way to the complete eradication of this pathology (Giordani et al. 2016). The treatment of HAT, diversified

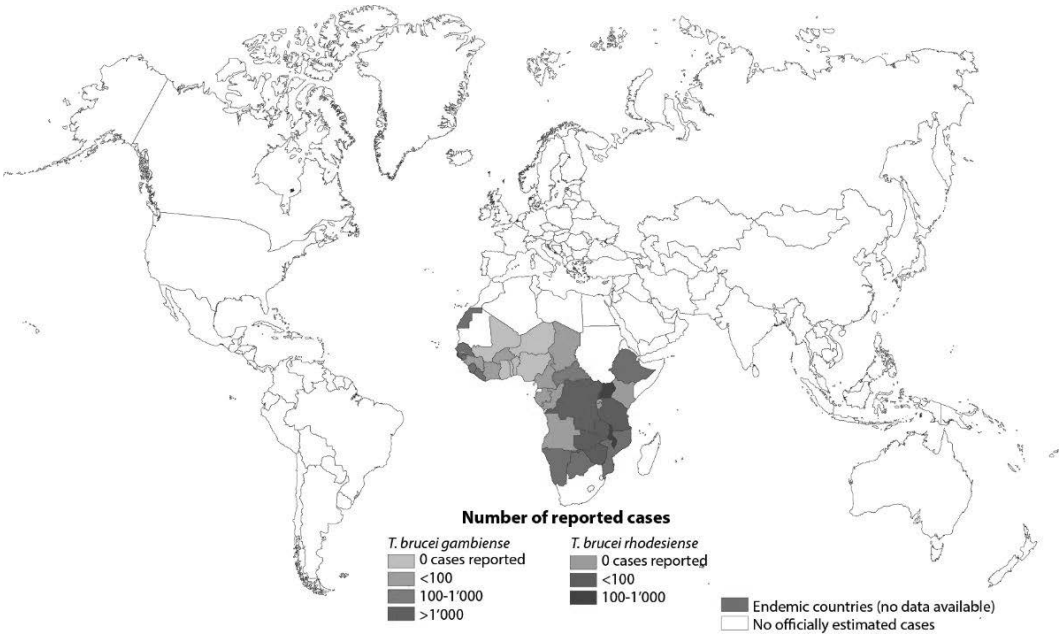

Figure 3. Distribution of Human African Trypanosomiasis (*T. b. gambiense* in green and *T. b. rhodesiense* in blue) worldwide. Adapted from WHO 2017.

Color version at the end of the book

depending on the stage of infection, is only based on chemotherapy (Cullen and Mocerino 2017). Nowadays, only four drugs and one drug combination are employed in therapy (Figure 2). Pentamidine is currently the first-line option for treating the initial stage of HAT (Sands et al. 1985) whereas suramin is employed as second choice or for the primary treatment of *T. b. rhodesiense* infection, for which it is more effective than pentamidine. However, both drugs suffer from important limitations: they are administered *via* injection, require a healthcare professional, are ineffective in stage two and, more importantly, have adverse side effects that are often responsible for the suspension of the treatment. Melarsoprol, eflornithine and nifurtimox, instead, are the only drugs actually effective in the second stage of HAT (Eperon et al. 2014). Melarsoprol was the first drug to be developed for HAT; it has been medically used since 1949 and it has the great advantage of being effective against both *T. b. gambiense* and *rhodesiense* infections. However, it derives from arsenic which is the reason for its undesirable effects, including fatal encephalopathy (Fairlamb et al. 2018).

Eflornithine is the only recent drug approved for HAT in 2000. It is a less toxic alternative to melarsoprol, even though it is completely ineffective against *T. b. rhodesiense*. The main drawback of eflornithine is the complex regimen of intravenous infusions 4-times per day for 14 days of treatment (Chappuis et al. 2005). Today eflornithine is rarely used alone and is normally prescribed in combination with nifurtimox. Nifurtimox alone is less effective against *T. brucei* than *T. cruzi*, but in combination with eflornithine, the efficacy of the treatment is comparable to that of eflornithine alone, but with considerably fewer side-effects than the monotherapy. In addition, the regimen of eflornithine in combination with nifurtimox is more manageable, furthermore permitting an oral administration of the two drugs (Priotto et al. 2009).

HAT and Chagas Diseases' Social Impact and Intervention

Although one seventh of the world's population has an interest in or is exposed to the risk of NTDs, these pathologies remain neglected at several levels. At the local level, they are usually not mentioned by

affected people, who are afraid of bias and marginalisation by the community. These pathologies barely spread outside the tropical area of origin; they do not represent an immediate risk for the 'occidental' countries that tend to be disinterested. However, the price to be paid for these choices is high: the NTDs have an elevated impact on the life of every single person, family and community, drastically decreasing the quality of life, aggravating poverty and reducing productivity - therefore representing a barrier for the economic growth of already depleted countries (Weiss 2008). Notwithstanding the social and economic burden, research and development for these illnesses is limited. For example, among all the 1,393 new drugs approved between 1975 and 1999, only 13 (0.9%) were targeted for NTDs, and only four of those were developed by pharmaceutical companies. The other nine were discovered as a result of veterinary and military research (Trouiller et al. 2002). Therefore, in order to encourage the research and development of new drugs that could be more effective, safe and economically sustainable, and to overcome the lack of interest of the major pharmaceutical companies in this health issue, associations between public and private institutions (PPP, public-private partnership) were recently initiated (Liese et al. 2010). These include the European Commission (Pierce et al. 2017) and other government agencies, private foundations and pharmaceutical multinationals such as the Drugs for Neglected Diseases Initiative (DNDi) (Chatelain and Ioset 2011) and the Medicines for Malaria Venture (MMV 2018). These PPPs coordinate the basic research conducted by universities and public health organizations with the experience and technology of the chemical and technological pharmaceutical industries to develop new drug candidates. The DNDi, along with partners including the Bill & Melinda Gates Foundation (WA, USA), Sanofi (Paris, France) and Médecins Sans Frontières (Geneva, Switzerland) are attempting to address the deficiency in accessible treatments and currently have two oral candidates in clinical trials. Acoziborole (SCYX-7158) emerged as a safe and promising candidate in late 2009 for the treatment of the second stage of HAT (Eperon et al. 2014). After successful preclinical trials, the drug entered clinical development in 2012, becoming a new chemical entity discovered by DNDi's lead-optimization program. In 2016, acoziborole entered into a Phase II/III clinical trial, which is expected to be completed by April 2020 (Jacobs et al. 2011). Fexinidazole, discovered by DNDi in 2005, is currently the most advanced oral drug candidate being developed for first stage and early second stage HAT (Eperon et al. 2014). A pivotal Phase II/III trial was completed in 2016, although two additional 'plug-in' trials are currently ongoing to assess the efficacy of the drug in special population groups not examined in the initial cohort. In addition, DNDi is also running a Phase III trial examining the effectiveness of fexinidazole in patients treated on both an out-patient basis and in a clinical hospital setting—depending on status. These trials are going to be completed by March 2020 (Mesu et al. 2018). Besides acoziborole and fexinidazole, which are two successful examples of new chemical entities identified for the treatment of trypanosomatidic infections, new drug candidates continuously enter the drug discovery pipeline.

Drug Discovery Approaches

Usually, the drug discovery for NTDs is carried out using classical ligand-based approaches, target-based approaches and phenotypic screening. Ligand-based approaches, which are discussed later in the chapter, are typically focused on the implementation of already known active compounds, natural compounds or drugs in therapy. Chemical structure modifications are then applied on the basis of classical medicinal chemistry strategies (Wermuth et al. 2015). Target-based approaches involve screening a library of compounds against a protein target and then optimizing the compounds for potency against the enzyme, selectivity, cellular activity, and pharmacokinetic properties. However, there are relatively few validated drug targets across the trypanosomiatidic infections (Frearson et al. 2007). Targets of major interest in the field of drug discovery are reported in Gilbert et al. (2013) and, in this chapter, we describe the main achievements in the fields of ergosterol biosynthesis, folate metabolism, phosphodiesterases, cysteine proteases and trypanothione metabolism. On the other hand, phenotypic screening has the advantage of identifying compounds that are active against the whole cell, meaning issues such as cell uptake and cell efflux have already been addressed (Haasen et al. 2017). There has been a major emphasis on phenotypic approaches to drug discovery for neglected diseases and a number of notable successes have been reported,

like the above mentioned fexinidazole and acoziborole (Eperon et al. 2014). Nonetheless, a balanced portfolio of carefully selected ligand- and target-based approaches together with phenotypic approaches is probably the best strategy for drug discovery for neglected tropical diseases. This must be complemented by studies in animal models, which are reviewed in the final section of this chapter.

Synthetic compounds active against Trypanosoma cruzi and Trypanosoma brucei

Over the years, numerous papers have been published aiming at new, more effective and safe drugs with fewer side effects. In the context of this chapter, the synthesis and SAR studies of compounds with interesting biological activity are described, covering related literature from 2010 to the present.

Quinoline derivatives

A series of 10 2-alkylaminomethylquinoline derivatives were synthesized (Muscia et al. 2011) and were tested against different developmental stages of *T. cruzi* (epimastigotes, trypomastigotes and amastigotes).

The interesting antiparasitic activity *in vitro* against epimastigotes of 5 compounds (IC_{50} = 3.4–11.8 μM vs 5.8 μM for benznidazole) led to further evaluation against trypomastigotes and amastigotes. Compound **1** was the most active against trypomastigotes with IC_{50} = 3.1 μM, with cytotoxic activity against COS-7 line slightly better than the reference drug (CC_{50} = 770.9 μM vs 706 μM for benznidazole). Furthermore, compound **1** showed good selectivity for both trypomastigotes and amastigotes with SI values of 248.7 and 60.2, respectively.

Reid et al. (2011) described the synthesis of derivatives of *N*-benzyl-1,2-dihydroquinolin-6-ols (Figure 5) and their evaluation against *T. brucei rhodesiense* STIB900. The authors proceeded with an extensive SAR study in order to decipher the effect of the substituents on the biological activity. These studies are summarized in Figure 6. The most active compounds *in vitro* were **2**, **3**, **4** and **5** with IC_{50} values 0.012 ± 0.001, 0.011 ± 0.001, 0.013 ± 0.004 and 0.014 ± 0.004 μM, respectively. These compounds were selected for *in vivo* evaluation and were administered to mice infected with *T. brucei rhodesiense* STIB900. Compound **2** suppressed parasitemia but a relapse occurred after 12.75 days after injection. Conversely, the ester prodrug **3** and the hydrochloride salts **4** and **5** resulted in cure even though at higher dosages (4 days × 50 mg/kg ip) than the reference drugs diminazene (4 days × 10 mg/kg ip) and pentamidine (4 days × 5 mg/kg ip).

Hiltensperger et al. (2012) described the synthesis of a library of quinolone-type compounds bearing a benzamide function in position 3 and an amine heterocycle in position 7 (Figure 7) for SAR purposes. These compounds were tested against *T. b. brucei* and *T. b. rhodesiense.*

In the context of the SAR studies, synthetic intermediates were tested as well. It is apparent that the amidation at position 3 is essential for activity but only for benzylamide and not for phenylamide derivatives, indicating the necessity for flexibility in position 3. In addition, the presence of cyclic and acyclic amines at position 7 enhances the activity. The most potent compound proved to be compound **6** which exhibited promising *in vitro* activity against *T. brucei* (IC_{50} = 47 nM) and *T. b. rhodesiense* (IC_{50} = 9 nM) combined with low cytotoxicity against macrophages J774.1. Hence, compound **6** was chosen for *in vivo* evaluation in a murine model of HAT. A preliminary formulation for oral administration was developed but was unsuccessful against *T. b. rhodesiense* (STIB900) infected NMRI mice.

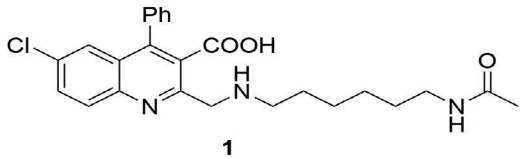

1

Figure 4. Structure of the 2-alkylaminomethylquinoline derivative **1**.

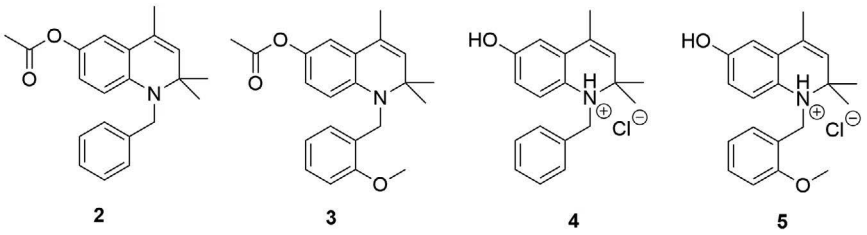

Figure 5. Structures of most active *N*-benzyl-1,2-dihydroquinolin-6-ols **2–5**.

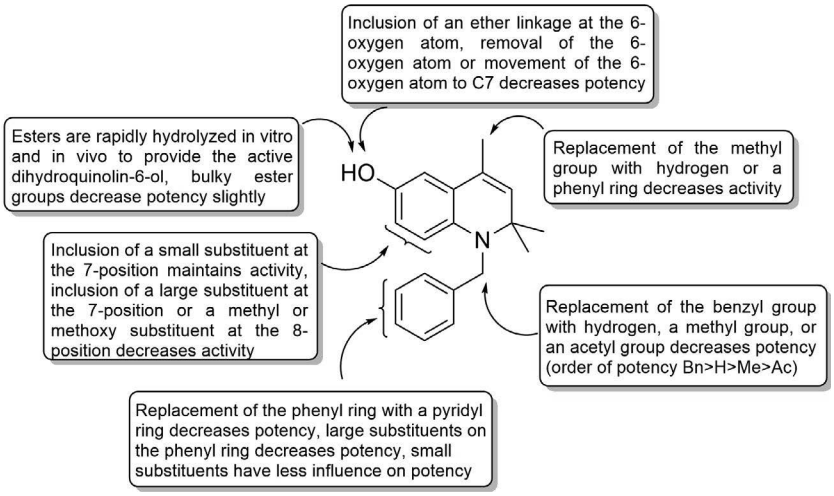

Figure 6. Activity map of tested compounds (Reid et al. 2011).

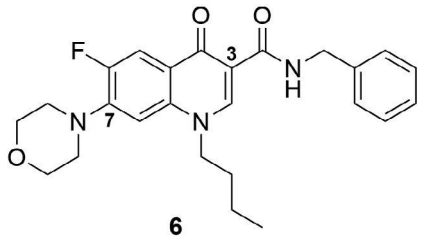

Figure 7. Structure of the most potent compound **6**.

Upadhayaya et al. (2013) described the synthesis of a series of compounds based on quinolines and indenoquinolines with variable side chains. From this library, five compounds (Figure 8) showed interesting activity. These compounds have shown better activity than benznidazole and nifurtimox (IC_{50} = 0.25–0.65 μM) against *T. cruzi* and *T. brucei*.

A series of new 3-nitrotriazole and 2-nitrotriazole-linked quinolines and quinazolines were synthesized and their antitrypanosomal activity was tested (Papadopoulou et al. 2017). Even though almost all compounds showed activity against *T. cruzi* and *T. b. rhodesiense*, only 2 chloroquinoline derivatives (**12** and **13**, Figure 9) exhibited satisfactory selectivity indices.

Particularly, compound **12** which bears a nitroimidazole moiety showed IC_{50} values of 1.29 and 1.11 μM against *T. b. rhodesiense* and *T. cruzi,* respectively, while compound **13**, which bears a nitrotriazole moiety, showed IC_{50} values of 0.038 and 0.574 μM, respectively. Especially compound **13** exhibited an excellent selectivity index against *T. b. rhodesiense* (SI = 1937).

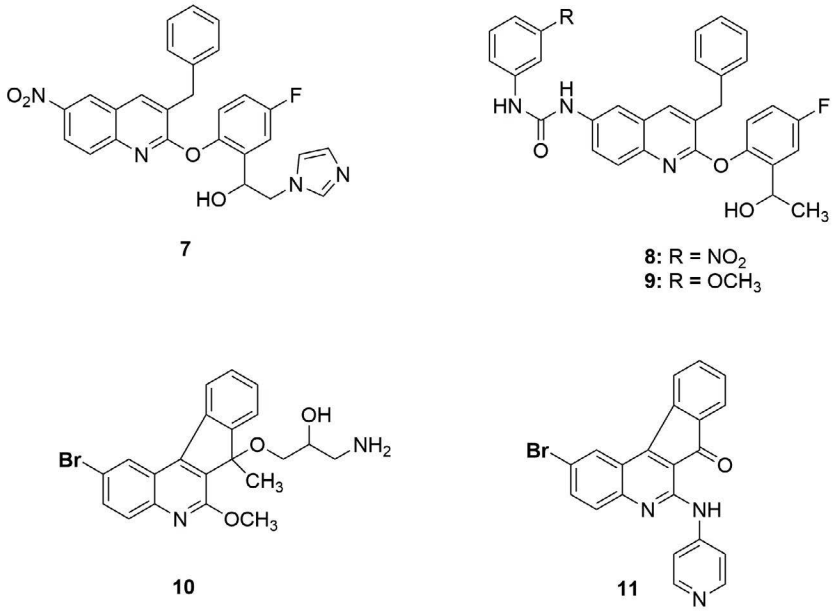

Figure 8. Structures of quinoline (**7–9**) and indenoquinoline (**10**, **11**) derivatives.

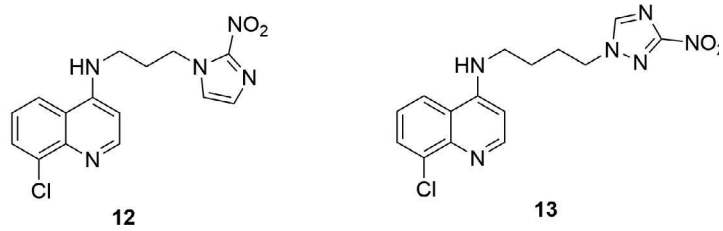

Figure 9. Structures of most potent chloroquinolines **12** and **13**.

Diamines and polyamines

Caminos et al. (2012) described the synthesis of 25 *N,N*'-disubstituted diamines through reductive amination of free aliphatic amines with various substituted benzaldehydes. This library was screened for antiparasitic activity *in vitro* against *T. brucei* and *T. cruzi.* In terms of SAR studies, the length of the aliphatic chain between the two amino functions was studied as well as the substitution of the benzyl moiety attached to the amines. The most promising compounds were **14** and **15** that bear a 4-OBn substitution and the aliphatic chain comprises 3 or 4 carbons (Figure 10). These compounds exhibit medium activity against *T. cruzi* (IC_{50} = 0.78 and 0.76 μM, respectively); however, they are significantly more active against *T. brucei* (IC_{50} = 0.062 and 0.097 μM, respectively) and with higher selectivity indices (SI = 97 and 60, respectively).

Sánchez-Moreno et al. (2012) published the synthesis of four pyrazole-containing macrocyclic and macrobicyclic polyamines and their *in vitro* and *in vivo* evaluation as potential antichagasic agents. Two of these compounds, **16** and **17** (Figure 11), were the most active from the compounds tested in *T. cruzi* epimastigote, axenic amastigote and intracellular amastigote forms. In addition, they proved to be more active than the reference drug benznidazole. More specifically, compound **16** showed an IC_{50} = 1.3 ± 0.1 μM and compound **17** showed an IC_{50} = 1.3 ± 0.3 μM (versus benznidazole IC_{50} = 15.9 ± 1.1 μM) against the epimastigote form. Concerning the axenic epimastigote form, the IC_{50} values for compounds **16** and **17** were 7.2 ± 2.2 μM and 8.8 ± 1.8 μM, respectively (benznidazole IC_{50} = 15.9 ± 1.1 μM). Finally, the

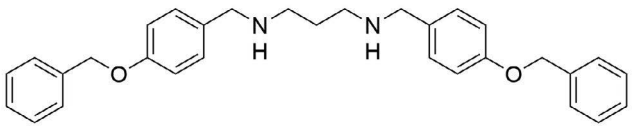

14

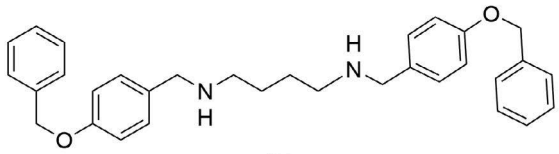

15

Figure 10. Structures of the most potent diamines **14** and **15**.

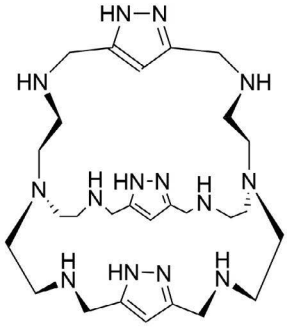

16

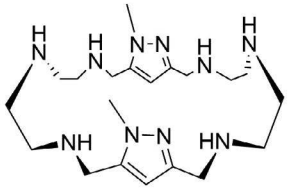

17

Figure 11. Structures of macrobicyclic and macrocyclic pyrazole-containing polyamines **16** and **17**.

IC_{50} values for compounds **16** and **17** were 6.2 ± 0.8 μM and 6.5 ± 1.6 μM, respectively, against the intracellular amastigote form, while for benznidazole, it was 23.3 ± 4.6 μM. Regarding the cytotoxicity evaluation, compounds **16** and **17** were substantially less toxic than the reference drug (IC_{50} = 149.1 and 178.5 μM, respectively, against 13.6 μM for benznidazole).

Prompted by the *in vitro* results, these compounds were tested *in vivo* against female BALB/c mice and they proved to be more active than benznidazole in both the acute and chronic phase animal models.

Acridones

A small library of acridones was synthesized and their antiparasitic activity was tested (Montalvo-Quirós et al. 2015). The most active compounds are depicted in Figure 12. Acridones **18–20** showed excellent activity against *T. b. rhodesiense* (IC_{50} = 0.069, 0.007 and 0.062 μM, respectively), accompanied by very good selectivity (SI > 2000). The *N*-methylation of these compounds to the corresponding acridones **21–23** did not alter the activity of **22** and **23** but increased the activity of **21** 10-fold (IC_{50} = 0.007 μM).

Compounds **18–20** were chosen for preliminary *in vivo* evaluation in the *T. b. rhodesiense* mouse model. Compound **19** confirmed its activity since three out of four mice were cured, with mean day of relapse over fifty days.

Thiohydantoins

During a high throughput screen for potential inhibitors of *T. brucei in vitro*, Buchynskyy et al. (2017a) discovered the substituted 2-thiohydantoin **24** (EC_{50} = 346 nM) as a potential hit compound. An extensive

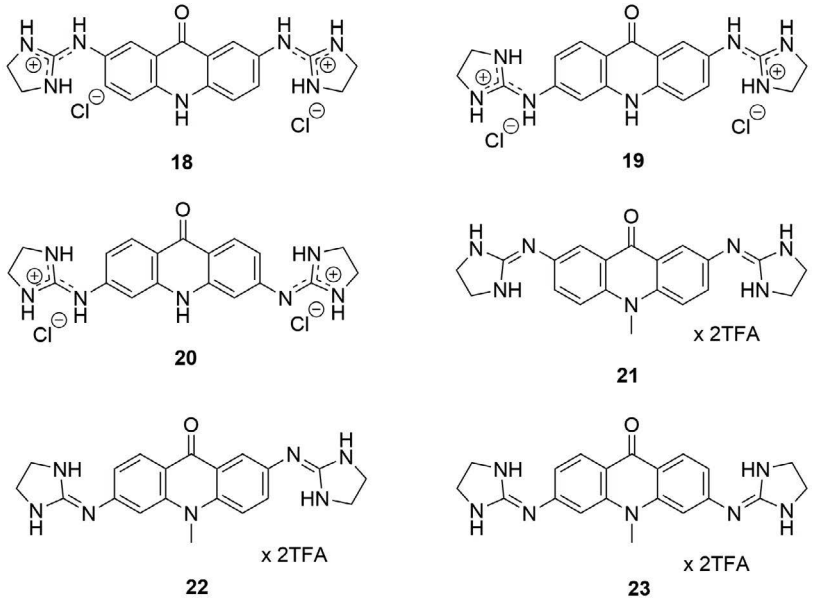

Figure 12. Acridones **18–23** with activity against *T. b. rhodesiense*.

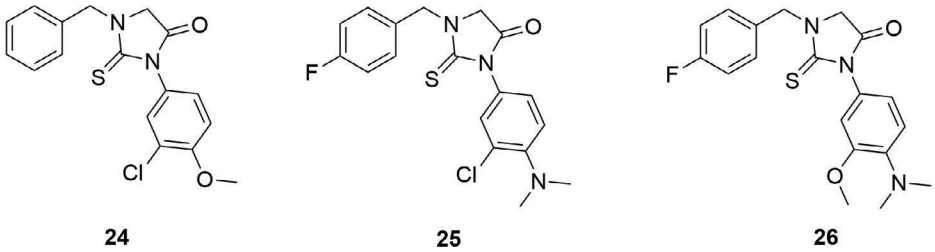

Figure 13. Hit compound **24** and lead compounds **25** and **26**.

SAR study which comprised changes to each of the phenyl moieties in terms of lipophilicity, site of substitution, electron donating and electron withdrawing groups and the combination of them, led to two new compounds **25** and **26** (Figure 13). These compounds showed excellent *T. brucei* activity *in vitro* (EC_{50} = 3 nM for **25** and EC_{50} = 2 nM for **26**). For this purpose, they were also tested *in vivo* in the acute phase model of HAT. Both compounds cured all treated mice as no parasitemia was detected for 60 days after infection.

Quinones, quinoxalines and quinazolines

In recent years, naphthoquinone has drawn much attention as a scaffold with potential antitrypanosomatidic activity. Carneiro et al. (2012) reported the synthesis of new oxirane derivatives using naphthoquinones as starting materials. Even though most of the synthesized compounds proved more active than the reference drug benznidazole (IC_{50} = 11.5 μM, CC_{50} = 48 μM) in epimastigote forms of *T. cruzi*, only compound **27** (Figure 14) exhibited comparable cytotoxicity (IC_{50} = 0.09 μM, CC_{50} = 44 μM).

Khraiwesh et al. (2012) synthesized 11 new imido-substituted 1,4-naphthoquinones which were tested against *T. cruzi* epimastigotes. Interestingly, all compounds showed better activity (IC_{50} = 0.7–6.1 μM) than the reference drug nifurtimox (IC_{50} = 10.67 μM, SI = 10.86) but only 4 of them, compounds **28**–**31** (Figure 15), exhibited a higher selectivity index (SI = 31.83–275.3).

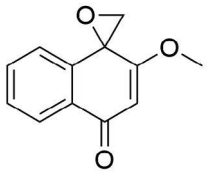

27

Figure 14. Structure of the most active oxirane derivative **27**.

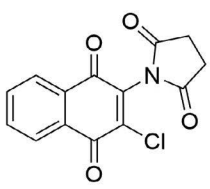

28

IC_{50} = 2.77 μM, SI = 60.25

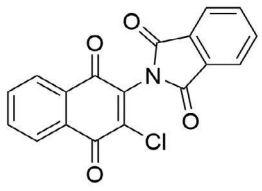

29

IC_{50} = 4.83 μM, SI = 53.97

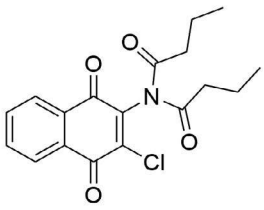

30

IC_{50} = 0.70 μM, SI = 31.83

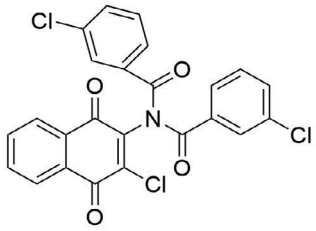

31

IC_{50} = 2.23 μM, SI = 275.3

Figure 15. Structures of the most active imido-substituted 1,4-naphthoquinones **28–31**.

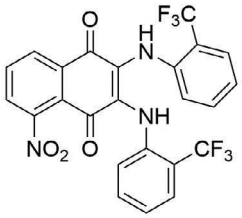

32

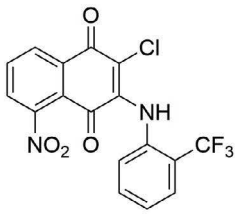

33

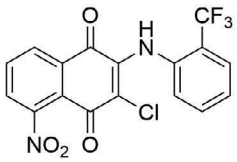

34

Figure 16. Structures of the most active mono- and di-substituted naphthoquinones **32–34**.

Samant and Chakaingesu (2013) synthesized a series of mono- and disubstituted naphthoquinones and all compounds were tested against *T. b. rhodesiense*. The most promising compounds are depicted in Figure 16. The monosubstituted compounds **33** and **34** were more active (IC_{50} = 0.07 ± 0.01 μM and 0.05 ± 0.01 μM, respectively) than the disubstituted one (**32**) (IC_{50} = 0.09 ± 0.01 μM). In addition, these three compounds (**32–34**) were the least cytotoxic from this library, exhibiting values 88 ± 5 μM, 75 ± 5 μM and 95 ± 5 μM, respectively, when tested against L-6 rat skeletal myoblast cells.

A new library of aryloxy-quinone derivatives was synthesized (Vásquez et al. 2015). Interestingly, almost all new compounds were more active against *T. cruzi* epimastigotes and with better selectivity

index on murine macrophages J-774 cells than the reference drug nifurtimox (IC_{50} = 7.00 ± 0.3 μM, SI = 40). However, the combination of activity and selectivity led to four potential hits (Figure 17). Compound **35** was the most active (IC_{50} = 0.02 ± 0.01 μM, SI = 625) followed by compounds **36–38** with IC_{50} values 0.05 ± 0.02 μM, 0.04 ± 0.02 μM and 0.09 ± 0.04 μM, respectively.

In the last decade, quinoxaline derivatives have been characterised as potential anti-trypanosomatid agents (Ancizu et al. 2009). Numerous compounds have been synthesized and evaluated and thus, some structural requirements have been established against trypanosomatids *in vitro*. Hence, the main structural requirements comprise the existence of the *N*-oxide moiety and the insertion of electron withdrawing groups on the quinoxaline ring.

Benitez et al. (2011) synthesized an extensive library of quinoxalines *N,N'*-dioxides as potential anti-*T. cruzi* agents. Initially, the evaluation of these compounds was realized *in vitro* against the epimastigote form of the Talahuen 2 strain of *T. cruzi* by calculating the percentage of growth inhibition (PGI). The most active compounds were **39–47** (Figure 18). In addition, the ID_{50} concentrations (50% inhibitory dose) were assessed with the most active compounds being **39** (ID_{50} = 0.4 μM), **40** (ID_{50} = 0.7 μM) and **42** (ID_{50} = 0.39 μM). Active compounds were also tested against two other *T. cruzi* strains, namely, colombiana and Y strains. In particular, the most potent compounds, **40** and **42,** were tested *in vivo* in murine models of acute Chagas' disease against the bloodstream trypomastigote form of *T. cruzi*, the CL Brener clone showing a very interesting biological profile.

The aforementioned structural prerequisites concerning quinoxalines were confirmed by Torres et al. (2013). 18 new quinoxaline *N,N'*-dioxides were synthesized and evaluated against the epimastigote form of the Talahuen 2 strain of *T. cruzi* by calculating PGI. 14 out of 18 compounds showed PGI values of 100% while the most active compounds were **48–53** (Figure 19) with IC_{50} values varying from 0.4–2.6 μM. Compound **52** was the most active compound (IC_{50} = 0.4 μM).

Patel et al. (2013) described a repurposing effort for the approved human cancer drug lapatinib (**54**) towards the discovery of more potent growth inhibitors of *T. brucei*. After an extensive SAR study, 4-anilinoquinazoline **55** (NEU-617) emerged as the most potent, orally bioavailable inhibitor of trypanosome replication (Figure 20). All compounds were tested against cultures of *T. brucei brucei* Lister 427. Compound **55** (EC_{50} = 0.042 μM) was more active than lapatinib (EC_{50} = 1.54 μM) and it was even more selective against HepG2 cells (> 20 μM versus 6.2 μM for lapatinib).

Au.: Meaning?

In an effort to further optimize **55** (NEU-617) as an antiparasitic lead compound, Devine et al. (2015) proceeded with the synthesis of new derivatives involving several replacements on the quinazoline scaffold. Even though **55** was superior against *T. brucei* compared to the new derivatives, several hits were discovered against other protozoal species, i.e., *T. cruzi*, *L. major* and *P. falciparum*. Thus, compound **56**

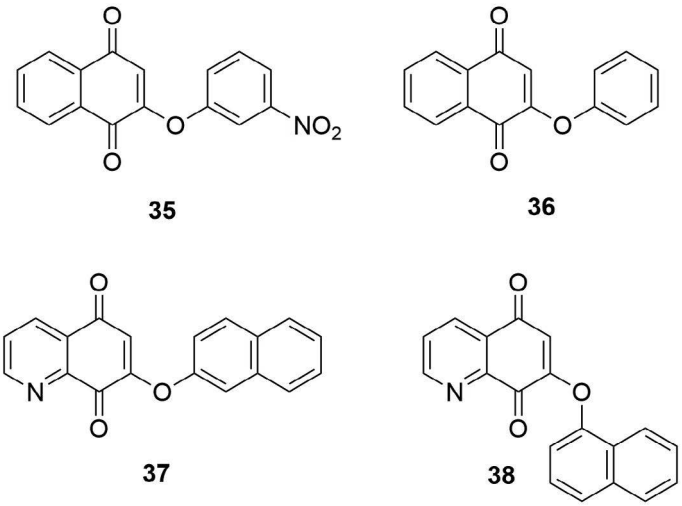

Figure 17. Structures of the most active aryloxy-quinones **35–38**.

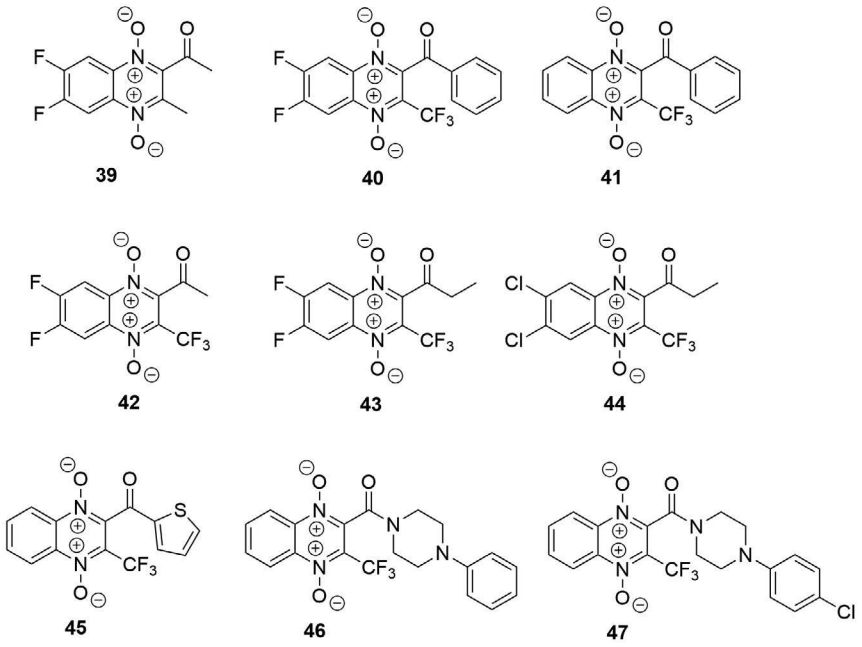

Figure 18. Structures of the most active quinoxaline *N,N'*-dioxides **39**–**47**.

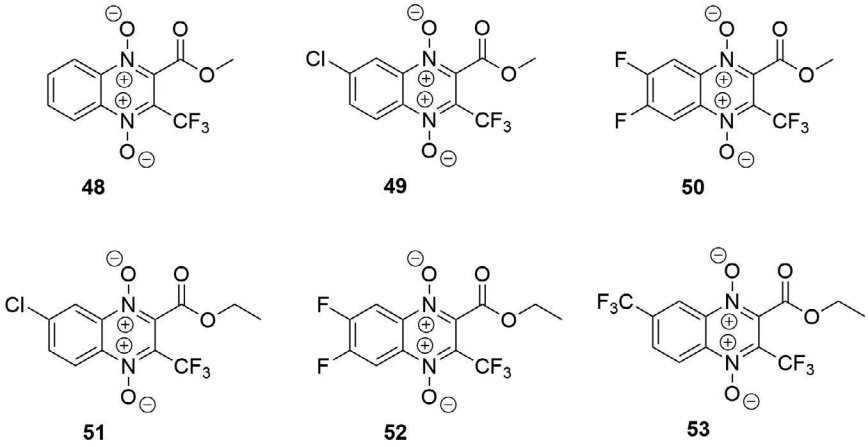

Figure 19. Structures of the most active quinoxaline *N,N'*-dioxides **48**–**53**.

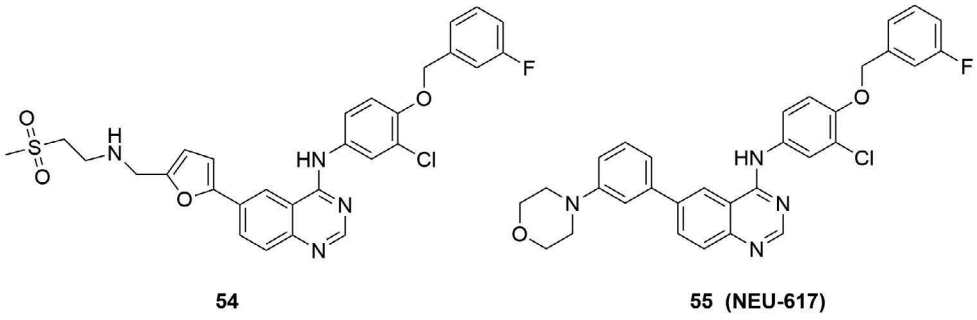

Figure 20. Structures of lapatinib (**54**) and the most potent inhibitor **55**.

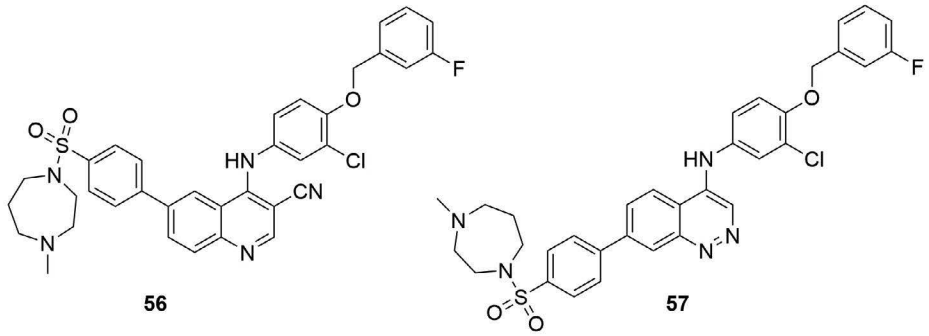

Figure 21. Structures of the most potent inhibitors **56** and **57**.

was found to be the most active compound against intracellular amastigotes of *T. cruzi* (EC_{50} = 0.09 μM) and compound **57** the most potent from the new library against *T. brucei* (EC_{50} = 0.21 μM) (Figure 21).

Benzamide derivatives

Based on their previous findings (Hwang et al. 2010), Hwang et al. (2013a) reported their optimization efforts for chloronitrobenzamides (CNBs). Compound **58** was found to be active against *T. b. brucei* (EC_{50} = 0.92 μM) and for that reason, a new SAR study was conducted which was aimed towards the discovery of new leads in which the chloronitrobenzamide moiety remained intact. Numerous compounds were synthesized and tested and finally compounds **59–61** were the most potent against *T. b. brucei* (EC_{50} = 0.006, 0.027 and 0.041 μM, respectively) (Figure 22).

In addition, these compounds were tested against two other species, *T. b. rhodesiense* and *T. b. gambiense.* All compounds showed activity against *T. b. rhodesiense* (EC_{50} = 0.013, 0.007 and 0.011 μM, respectively) as well as against *T. b. gambiense* (EC_{50} = 0.036, 0.002 and 0.001 μM, respectively). This fact indicates that there is no species variation concerning the sensitivity against CNBs. However, these compounds exhibited poor to modest solubility, an issue that should be addressed in their further development.

In an effort to reduce complexity and molecular weight and at the same time, improve the pharmacological properties of CNBs, Hwang et al. (2013b) synthesized a new library of compounds by replacing the chloronitrobenzamide moiety. Even though most of the compounds were inactive, one potential lead (compound **62**, Figure 23) was found which bears the 4-chloropyridine carboxamide moiety. This compound showed good activity against *T. b. brucei* (EC_{50} = 0.12 μM) and excellent activity against *T. b. rhodesiense* (EC_{50} = 0.018 μM) and *T. b. gambiense* (EC_{50} = 0.038 μM).

Pyridyl benzamides were further explored as potential anti-trypanosomatidic agents (Ferrins et al. 2014). An extensive SAR study was conducted based on hit compound **63** (IC_{50} = 3.03 μM). A large library was synthesized and tested against *T. b. brucei*, *T. b. rhodesiense* and *T. cruzi*. Compounds **64–68** (Figure 24) showed activity with IC_{50} values ranging between 0.41–1.1 μM against *T. b. brucei* and 0.045–0.64 μM against *T. b. rhodesiense*, with the most active compound being **65** (IC_{50} = 0.045 μM). However, all compounds were inactive against *T. cruzi*. These compounds with low molecular weight have favorable properties for further optimization and have a very good prediction for CNS penetration which is essential for treating second stage HAT.

In the context of a high throughput screening campaign of 87000 compounds against *T. b. brucei*, Rahmani et al. (2015) identified a new class of potential trypanocides, pyrazine carboxamides. This screening delivered a starting hit, compound **69** (EC_{50} = 0.49 μM) and subsequent SAR studies were conducted concerning structural changes around the core. Several compounds showed very good activity against *T. b. brucei* and *T. b. rhodesiense* but the most active compounds were **70** with EC_{50} values of 0.035 and 0.024 μM against *T. b. brucei* and *T. b. rhodesiense*, respectively and compound **71** with EC_{50} values 0.025 and 0.038 μM, respectively (Figure 25). Worth mentioning is that this class of compounds showed

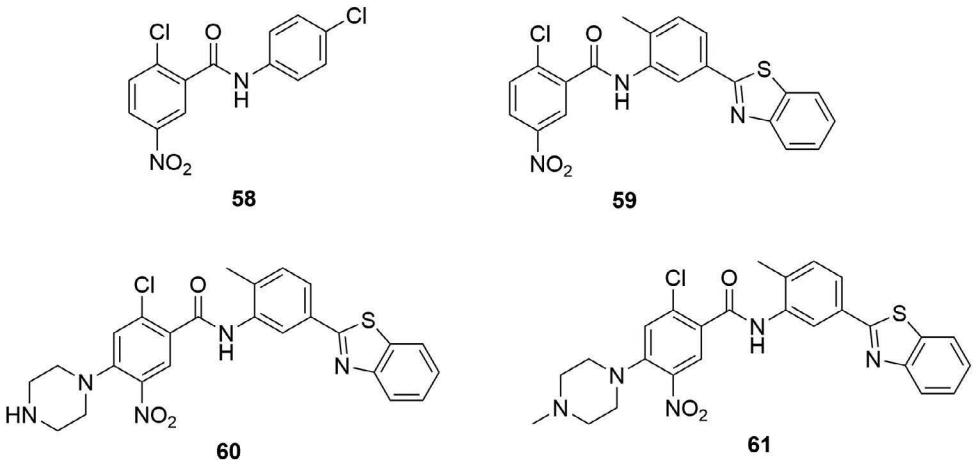

Figure 22. Structures of hit compound **58** and the most potent CNBs **59–61**.

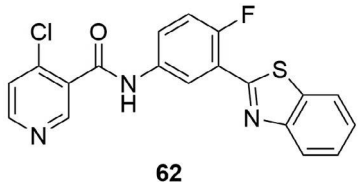

Figure 23. Structure of lead compound **62**.

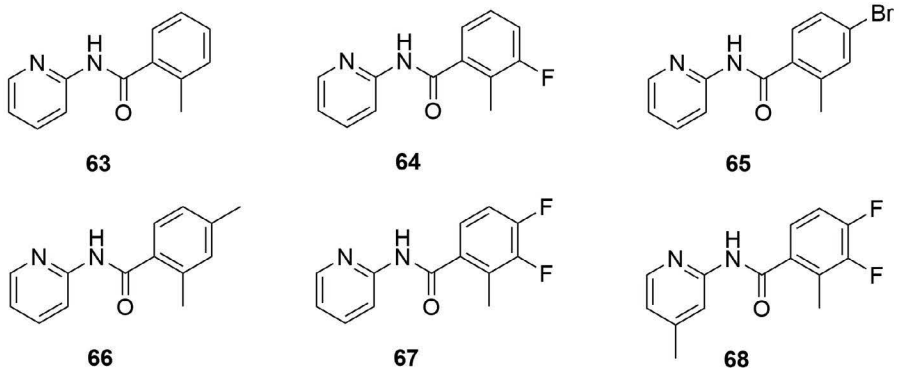

Figure 24. Structures of hit compound **63** and lead pyridyl benzamides **64–68**.

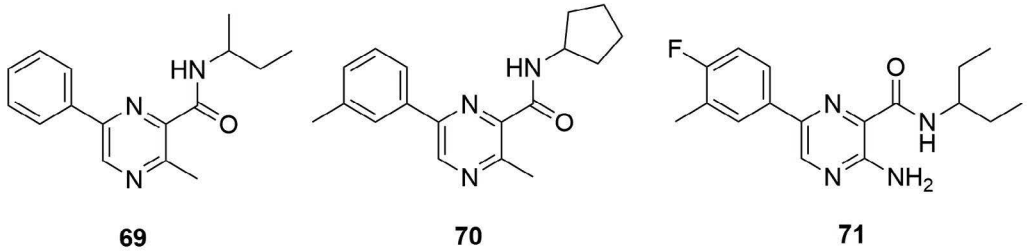

Figure 25. Structures of hit compound **69** and lead compounds **70** and **71**.

very low cytotoxicity and was selective for *T. brucei*, since no significant activity was observed against *T. cruzi*.

Cleghorn et al. (2015) conducted a phenotypic screening of compounds against *T. b. brucei* followed by a mammalian cell counterscreen (MRC-5 cells) to exclude nonselective compounds. This work led to indoline-2-carboxamide **72** (Figure 26) which showed good activity (EC_{50} = 27 nM) and selectivity over mammalian cells (> 1600 fold). With compound **72** in hand, SAR studies were realized in terms of core modifications and the effect of stereochemistry on the chiral center. These studies led to the discovery of two new compounds, **73** and **74** (racemic), with lower activity against *T. b. brucei* (EC_{50} = 60 and 80 nM, respectively) but with improved metabolic stability and enhanced *in vivo* exposure. These compounds exhibited excellent pharmacokinetic properties, and resulted in a full cure in a HAT stage 1 mouse model, but unfortunately only a partial cure in stage 2.

Buchynskyy et al. (2017b) identified *N*-(2-aminoethyl)-*N*-phenyl benzamides as an interesting class of compounds with potential antiparasitic activity against *T. brucei*. Compound **75** (Figure 27) was selected as a hit compound for its activity (EC_{50} = 1.21 μM) against *T. b. brucei*, its selectivity over mammalian cells (> 30 fold) and its drug-like features, including low molecular weight, clogP, H-bond donors and acceptors. The outcome of SAR studies was the discovery of some new lead compounds with EC_{50} values ranging from 0.001–0.031 μM with compound **76** being the most potent (EC_{50} = 0.001 μM against

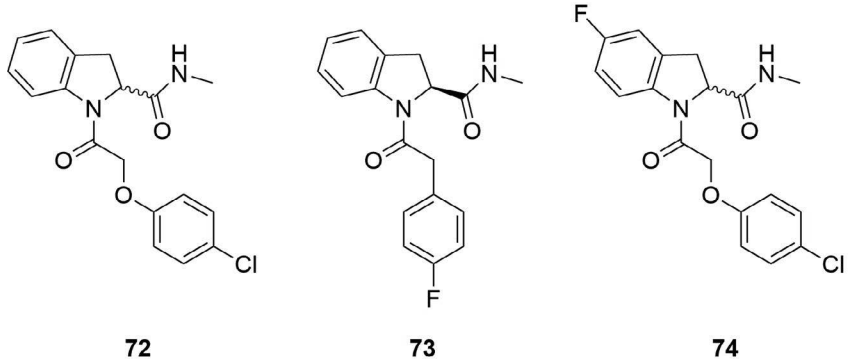

Figure 26. Structures of potent indoline-2-carboxamides **72–74**.

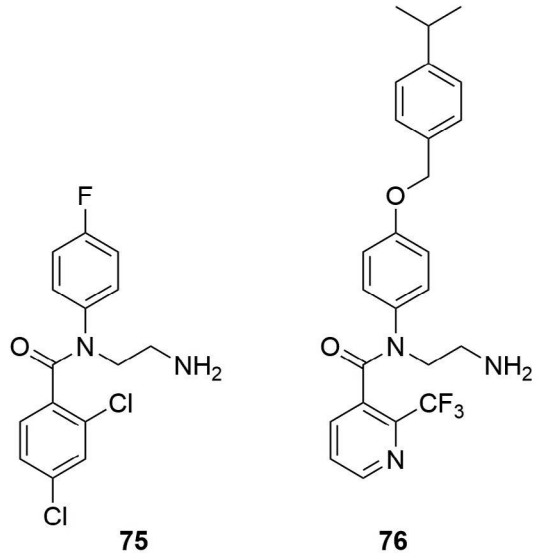

Figure 27. Structures of hit compound **75** and lead compound **76**.

T. b. brucei and 0.002 μM against *T. b. rhodesiense*). However, in murine efficacy models of HAT infection, the compounds showed only partial cures or suppression.

Chalcones

Chalcones form another class of compounds with broad spectrum pharmacological activities. Recently, Borsari et al. (2017) reported the synthesis of a library of thirteen 2-hydroxy chalcones bearing methoxy groups. All the synthesized compounds were tested against the bloodstream form of *T. brucei* and the intracellular *T. cruzi* at 10 mM. Compounds **77–79** (Figure 28) were the most potent against *T. brucei* with EC_{50} values 1.3 ± 0.02, 2.1 ± 0 and 2.1 ± 0.4 μM, respectively and with selectivity index > 12.

Bhambra et al. (2017) synthesized a small library of pyridylchalcones which were tested against *T. b. rhodesiense*. Even though none of these compounds showed better activity than the reference drugs pentamidine or melarsoprol, three compounds (**80–82)** can be considered as potential leads with IC_{50} values 0.29, 0.40 and 0.41 μM, respectively (Figure 29).

Hydroxamic acid derivatives

Fytas et al. (2011) discovered acetohydroxamic acids as a new class of compounds with potential antitrypanocidal activity. The synthesis of these compounds was realized through the attachment of an acetohydroxamic acid moiety to the imidic nitrogen of 2,6-diketopiperazines. A SAR study revealed that compounds **83** (S-enantiomer), **84** (R-enantiomer) and **85** (racemic mixture of **83** and **84**) (Figure 30) showed low nanomolar activity against bloodstream-form *T. brucei* with IC_{50} values 6.8 ± 1.4, 9.1 ± 0.2 and 17± 1 nM, respectively, while compound **83** along with compounds **86** and **87** displayed significant activity against *T. cruzi* with IC_{50} values 0.21 ± 0.04, 5.51 ± 0.68 and 3.62 ± 0.31 μM, respectively. Overall, compound **83** proved to be the most active compound against both species. In addition, these compounds showed very good selectivity indices. The fact that replacement of the hydroxamic acid moiety led to compounds with decreased activity makes this group a requisite for trypanocidal activity.

A small library of hydroxamic acid derivatives which inhibit human histone deacetylases was synthesized and tested against cultured bloodstream form *T. brucei* (Kelly et al. 2012). Most of these compounds exhibited very good activity in the submicromolar range. Specifically, the most promising compounds were **88–90** (Figure 31) with IC_{50} values 0.034 ± 0.002, 0.064 ± 0.005 and 0.086 ± 0.009 μM, respectively.

Thiazole derivatives

Zelisko et al. (2012) described the synthesis and biological evaluation of a series of 6,6,7-trisubstituted thiopyrano[2,3-*d*][1,3] thiazoles. Interestingly, one compound, **91** (Figure 32), inhibited *T. b. brucei* and

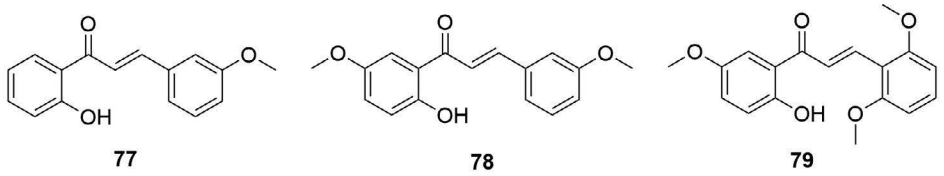

Figure 28. Structures of the most potent methoxylated 2-hydroxychalcones **77–79**.

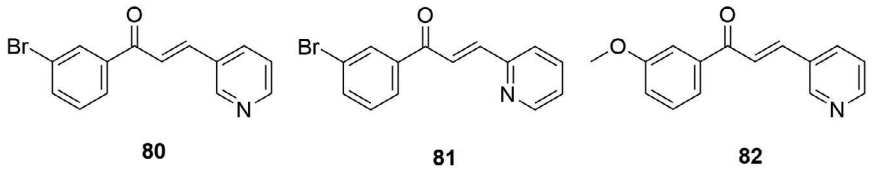

Figure 29. Structures of most potent pyridylchalcones **80–82**.

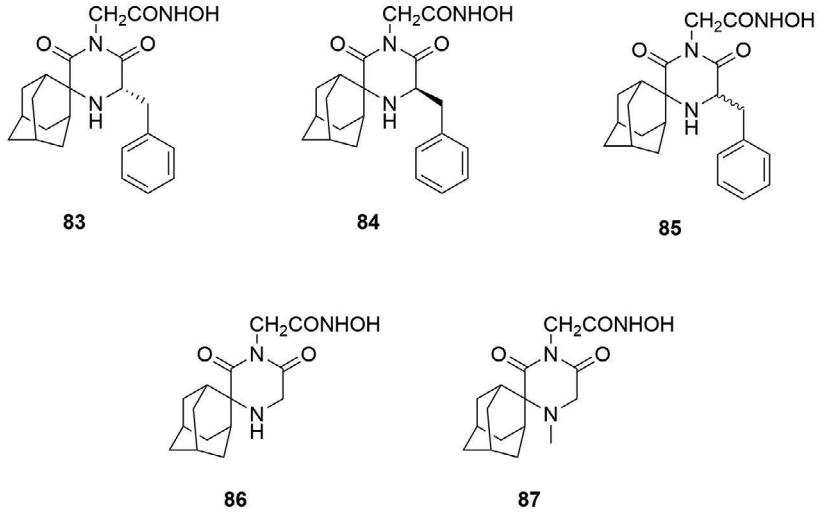

Figure 30. Structures of hydroxamic acids **83–87**.

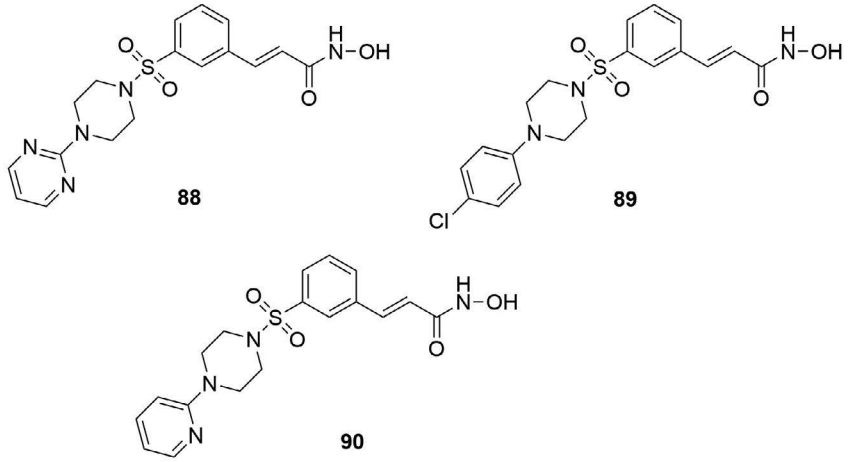

Figure 31. Structures of the most active hydroxamic acids **88–90**.

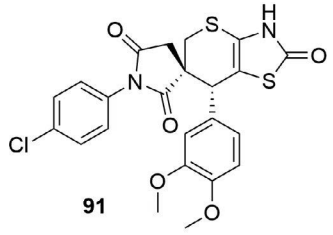

Figure 32. Structure of potential lead **91**.

T. b. gambiense with IC_{50} values 0.26 and 0.42 μM, respectively; thus, it can be considered as a potential lead for further optimization.

Cardoso et al. (2014) reported the synthesis and the anti-*T. cruzi* activity of 24 2-(pyridine-2-yl)-1,3-thiazoles by ultrasound-assisted synthesis. The majority of this class of compounds demonstrated better

activity than the reference drug benznidazole, with compounds **92** and **93** (Figure 33) being the most potent with IC_{50} values 1.2 μM each against *T. cruzi* trypomastigotes. In addition, this class of compounds showed no cytotoxicity against HepG2 cells.

Russell et al. (2016) published their work on hit to lead optimization of compound **94** (Figure 34). The latter emerged as a hit compound through a high-throughput screening because it exhibited interesting activity (IC_{50} = 0.80, 1.5 and 2.3 μM for *T. b. brucei*, *T. b. rhodesiense* and *T. cruzi*, respectively) and very good physicochemical properties. An extensive SAR study was conducted towards the discovery of new leads. Indeed, 2-(fluorophenyl)thiazole **95** was found to exhibit excellent activity against *T. b. brucei* (IC_{50} = 0.024 ± 0.003 μM, SI = 433) and *T. cruzi* (IC_{50} = 0.020 ± 0.01 μM, SI > 3162). Compound **95** was tested *in vivo* in Balb/c mice infected with the trypomastigote form of *T. cruzi Brazil* strain with encouraging results but unfortunately it was rapidly metabolized.

In a phenotypic high-throughput screening of 700,000 compounds, compound **96** (Figure 35) was identified, among others, as a potential inhibitor of *T. brucei* (IC_{50} = 0.632 μM, SI = 162 against *T. b. rhodesiense*). Patrick et al. (2016, 2017) with two back-to-back papers reported the efforts towards the optimization of a hit compound. A SAR study was conducted by focusing on changes to both phenyl rings of compound **96**. Therefore, 72 new derivatives were synthesized and tested against *T. b. rhodesiense* STIB900 and L6 rat myoblast cells for cytotoxicity *in vitro*. 44 compounds were more active than **96** and eight of them showed IC_{50} values below 100 nM. The most potent compound was **97** (IC_{50} = 9 nM, SI > 18,000) but unfortunately, the *in vivo* test showed that it was unable to cure infected mice. Even though the administration of **97** caused reduction of parasitemia, relapses occurred. This was attributed to poor metabolic stability. Prompted by these results, a second paper described a new SAR study of 65

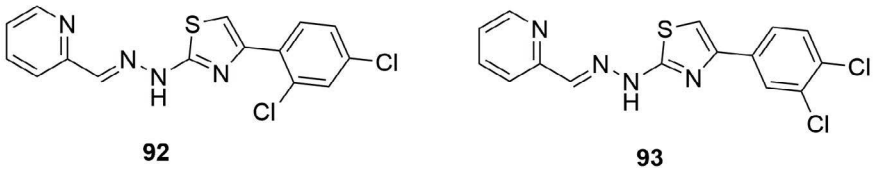

Figure 33. Structures of most potent thiazole derivatives **92** and **93**.

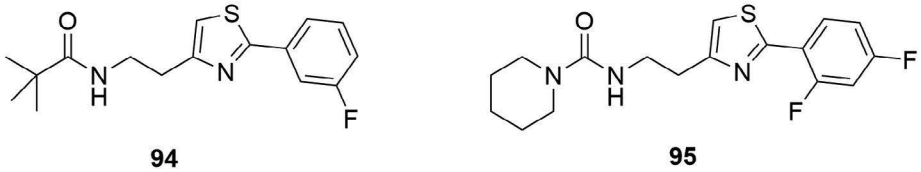

Figure 34. Structures of hit compound **94** and lead compound **95**.

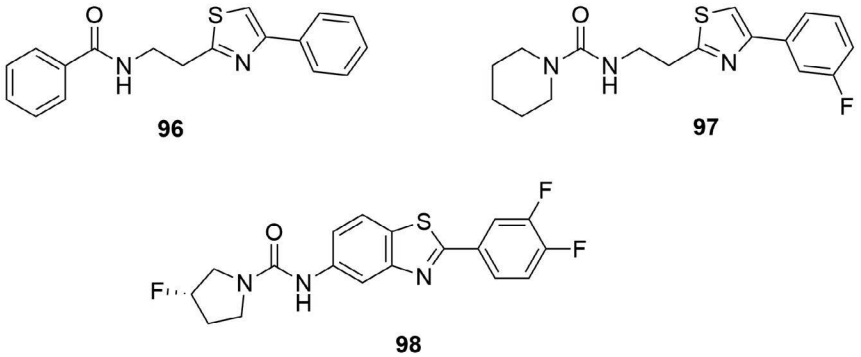

Figure 35. Structures of hit compound **96** and lead compounds **97** and **98**.

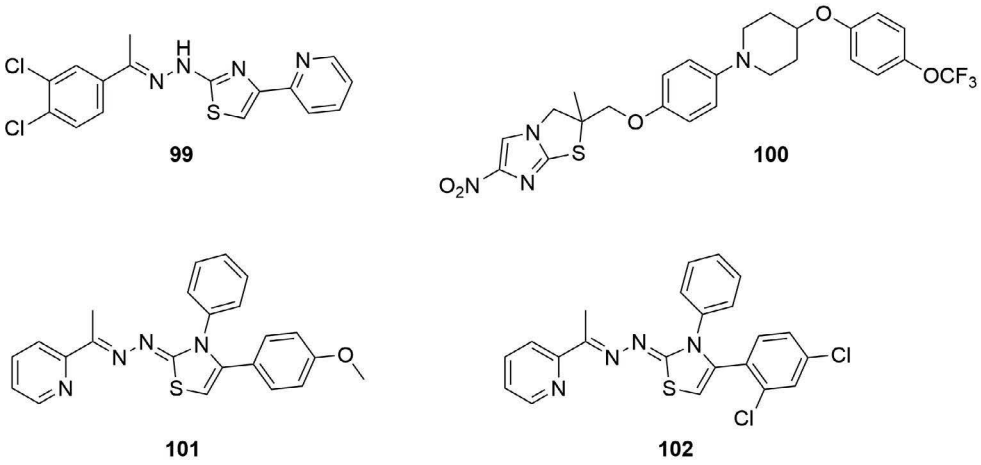

Figure 36. Structures of potential hits **99–102**.

additional compounds with modifications in other sites on hit **96** with the intention of maintaining the same activity and improving the metabolic stability. This led to compound **98** which was less active than **97** (IC_{50} = 35 nM) but with enhanced metabolic stability and brain penetration. Oral dosing of **98** cured five out of five mice in both acute and chronic murine models of HAT.

Many thiazole derivatives were synthesized and evaluated for their antiparasitic activity during the last year by several research groups. Compound **99** (Filho et al. 2017) showed activity against the promastigote form of *T. cruzi* (IC_{50} = 0.37 μM), compound **100** (Thompson et al. 2017) with IC_{50} = 0.055 μM against *T. cruzi*, and compounds **101** and **102** (Silva et al. 2017) with IC_{50} values 1.2 and 1.6 μM, respectively against the trypomastigote form of *T. cruzi* (Figure 36).

Au.: There are 2 refs for this year. Specify as a and b.

Thiophene derivatives

Bhambra et al. (2016) reported the synthesis of a small library of 2,6-disubstituted-4,5,7-trifluorobenzothiophenes. Compounds **103** and **104** (Figure 37) demonstrated interesting antitrypanosomal activity against *T. b. rhodesiense* with IC_{50} values 0.60 and 0.53 μM, respectively and no toxicity to mammalian cells. It is apparent that the activity of these compounds can be attributed to the existence of the benzimidazole moiety since its replacement resulted in loss of activity.

Indole derivatives

Vega et al. (2012) prepared a series of nitro-indazolin-3-ones which were tested *in vitro* against epimastigote forms of *T. cruzi*. Compounds **105–107** (Figure 38) showed interesting trypanocidal activity (IC_{50} = 0.93, 2.39, 1.17 μM, respectively) and low unspecified toxicity. The authors found structural similarities with other known antiprotozoan drugs during their search, and therefore they introduced a new scaffold for further research and optimization.

Tapia et al. (2014) synthesized a series of indole-4,9-dione and their activity was evaluated against the epimastigote form of *T. cruzi*, Y strain. All new compounds showed better activity and selectivity compared to the reference drug nifurtimox. Interestingly, compound **108** (Figure 38) demonstrated excellent nanomolar inhibitory activity (IC_{50} = 20 nM), and high selectivity index (SI = 625).

Imidazole derivatives

A high-throughput screening of 303,286 compounds revealed a class of imidazole-based inhibitors (**109–111**, Figure 39) that can inhibit infection of mammalian host cells by *T. cruzi* trypomastigotes (Bettiol et al. 2009). In an effort to further optimize the activity, cytotoxicity and bioavailability, new

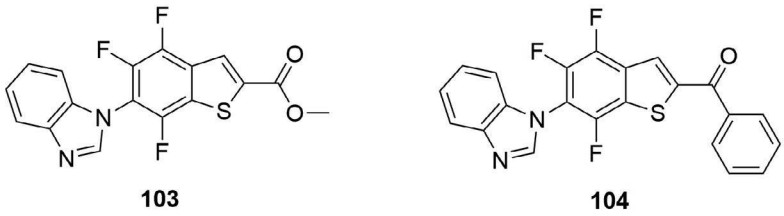

Figure 37. Structures of potential hits **103** and **104**.

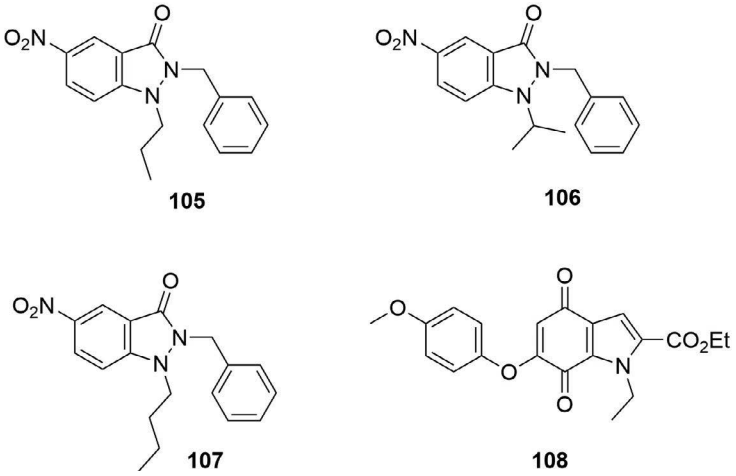

Figure 38. Structures of indole derivatives with potential trypanocidal activity.

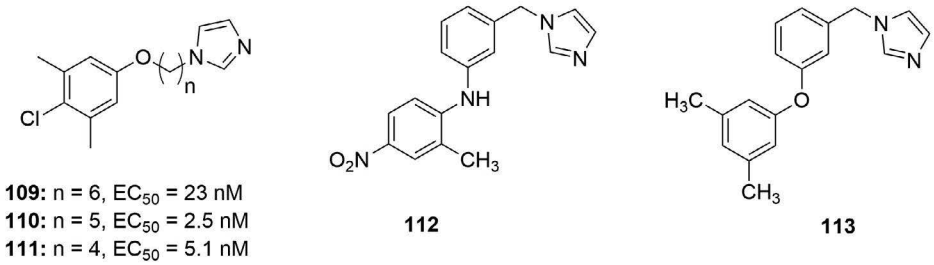

Figure 39. Structures of hit compounds **109–111** and lead compounds **112** and **113**.

inhibitors of *T. cruzi* CYP51 were synthesized (Andriani et al. 2013) with ring-constrained structures. The most promising inhibitors were **112** (EC_{50} = 72 nM) and **113** (EC_{50} = 80 nM).

The SAR study revealed that the substitution of the phenyl ring with lipophilic groups is essential. The absence of these groups was accompanied by loss of potency. In addition, replacement of the imidazole moiety by other nitrogen heterocycles, such as pyrazole or triazole, resulted in loss of activity. Hence, the presence of an imidazole ring is required for *T. cruzi* CYP51 binding.

More compounds bearing an imidazole ring have been synthesized and tested against the drug-targetable enzyme CYP51 due to structural similarities with its inhibitors. In particular, compounds **114–116** (Figure 40), even in their racemic form, showed very interesting biological activity against *T. cruzi* Talahuen C2C4 amastigote stage (Friggeri et al. 2013) with IC_{50} values 14, 5 and 36 nM, respectively. The authors wanted to further explore the activity of the single enantiomers which led to the conclusion that *S*-enantiomers were more active than the corresponding *R*-enantiomers. Compound **(*S*)-114**

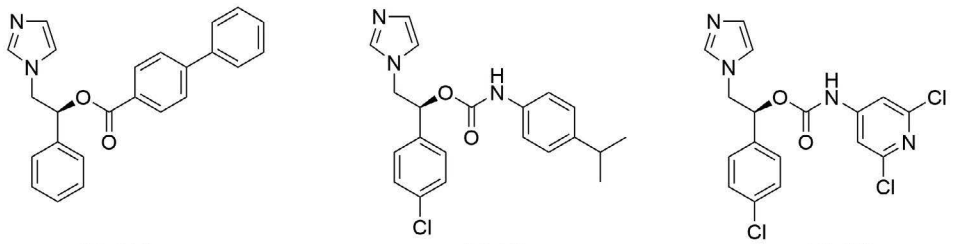

Figure 40. Structures of active compounds **114**–**116**.

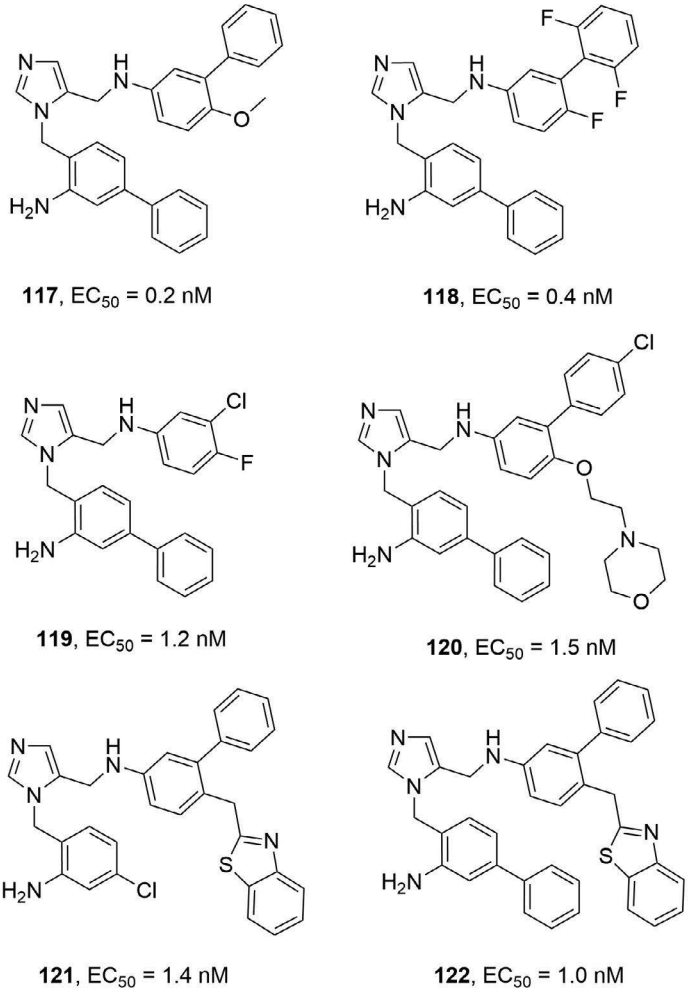

Figure 41. Structures of the most active dialkylimidazoles **117**–**122**.

showed IC_{50} = 3.8 nM vs 193 nM of **(*R*)-114**, **(*S*)-115** showed IC_{50} = 1.8 nM while **(*R*)-115** showed IC_{50} =112 nM and **(*S*)-116** showed IC_{50} = 23.6 nM vs 97.2 nM of **(*R*)-116**.

Suryadevara et al. (2013) described the synthesis of 75 dialkylimidazole-imidazole based inhibitors of CYP51. Interestingly, most of the compounds showed remarkable nanomolar activity against *T. cruzi* amastigotes. The most promising compounds and their EC values are depicted in Figure 41.

Computational and experimental structure-based drug design strategies against Trypanosoma cruzi and Trypanosoma brucei

In the above section, we presented a large number of synthetic compounds that have been optimized for their anti-trypanosomal properties; however, this was often done without taking specific molecular targets into account. Target-oriented methods provide an alternative strategy or can present an interesting complement to optimization based solely on anti-parasitic properties. In this section, we review some of the recent literature on structure-based drug design (SBDD) efforts to tackle trypanosomatidic infections by targeting specific metabolic pathways or enzymes that have been extensively explored in target-guided drug discovery approaches during the past years, such as CYP51, folate pathway proteins, phosphodiesterases, cysteine proteases or enzymes of the trypanothione metabolism. In the discovery of new hits and lead optimization, experimental methods and computational techniques are widely used together to facilitate the process of compound library design and iterative improvement in the context of known (or predicted) biomolecular targets. We describe approaches to SBDD for key targets, as well as techniques for tackling typical challenges in SBDD, such as selectivity, off-target binding and deciphering the mechanism-of-action (MoA) of a drug. We conclude the section with a brief summary of the methods typically employed in anti-trypanosomatidic drug discovery, their potential applications and limitations.

Compounds targeting the lanosterol 14α-demethylase (CYP51)

A particularly prominent example of a widely considered anti-trypanosomatid drug target is an enzyme involved in the ergosterol biosynthesis route, namely the lanosterol 14α-demethylase (or CYP51). CYP51s, which belong to the family of cytochrome P450s, are highly conserved heme-containing proteins involved in the production of plasma membrane building blocks and regulatory molecules (Lepesheva and Waterman 2004, 2007). Azole-based CYP51 inhibitors are known anti-fungal agents (Lass-Flörl 2011, Denning and Bromley 2015) and the trypanosomal ergosterol biosynthesis resembles that of fungi, making the repurposing of anti-fungal compounds a well-explored design strategy (Buckner and Urbina 2012). Furthermore, crystallographic complexes of TbCYP51 and TcCYP51 with anti-fungal compounds, such as fluconazole **123** and posaconazole **124** (Figure 42, Chen et al. 2010), paved the way for further optimization of azole-based and chemically distinct CYP51 inhibitors for trypanosomatidic infections. As another example, Hoekstra et al. (2015) reported the crystallographic complex of a 1-tetrazole-based anti-fungal clinical drug candidate with TcCYP51, providing an additional target-based starting point for future optimization of the compound as an anti-Chagas agent.

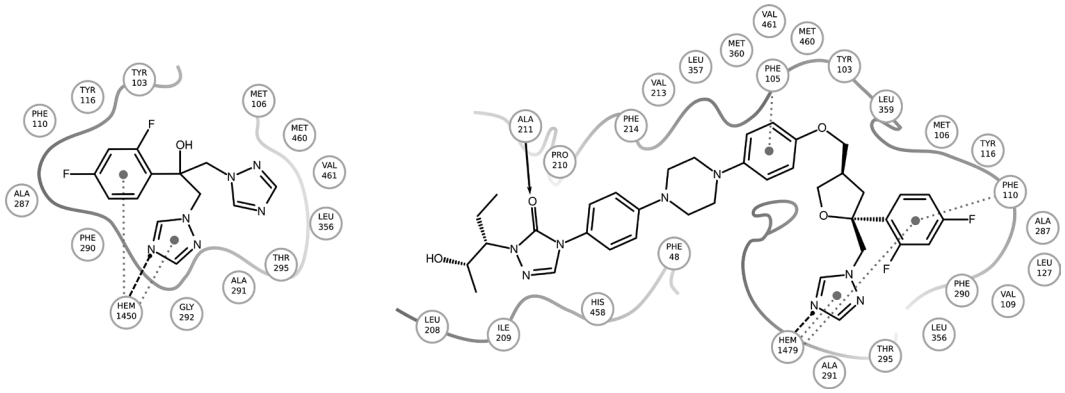

Figure 42. Interaction diagrams of the anti-fungal compounds fluconazole **123** (left) in TcCYP51 and posaconazole **124** (right) in TbCYP51. The diagrams are based on the crystallographic complexes with PDB-ID 2wuz and 2x2n (Chen et al. 2010), respectively. Pocket-lining residues and the pocket shape are shown. Black dashed lines indicate coordination bonds between the ferric heme iron and a nitrogen atom of the ligand, gray dotted lines indicate π-π interactions and black arrows indicate hydrogen-bonding interactions.

Hargrove et al. (2013) used X-ray crystallography to determine the binding modes of the promising pyridine-based drug candidates **125** and **126** (Figure 43) for Chagas disease. These compounds were found to be the first non-azole compounds showing potent inhibition of TcCYP51 as posaconazole **124**. Importantly, the structural data show that the coordination bond between the pyridine heterocycles of **125** and **126** and ferric heme iron of TcCYP51 are longer than in the case of azoles. The authors highlight that this may allow for achieving higher selectivity between the trypanosomal enzyme and the human variant since, due to the weaker coordinating interaction, the other non-bonded interactions between the protein and the ligand, which differ between the targets, become more important determinants for compound binding affinities. However, as can be seen in Figure 43, the interaction of compounds **125** and **126** with TcCYP51 is mainly mediated by hydrophobic contacts.

The development of the aforementioned imidazole-based *T. cruzi* CYP51 inhibitors **112** and **113** (see Figure 39) by Andriani et al. (2013) as well as compounds **114**–**116** (Figure 40) by Friggeri et al. (2013) was similarly supported by crystallographic data (directly by structure determination or indirectly by docking studies to existing crystal structures). In a follow-up study, Friggeri et al. (2014) further optimized imidazole-based inhibitors and demonstrated their ability to bind to CYP51 in two different regions: either in the substrate-binding site close to the heme group or in the substrate access channel (compare binding mode of **127** in Figure 44).

Another example of a particularly successful SBDD approach is the drug candidate (R)-N-(1-(3,4'-difluorobiphenyl-4-yl)-2-(1H-imidazol-1-yl)ethyl)-4-(5-phenyl-1,3,4-oxadiazol-2-yl)benzamide (**128**, Figure 45) developed by Lepesheva et al. (2015). Based on **127**, which cured both acute and chronic Chagas disease in experimental models, and the existing structural knowledge for CYP51 (Lepesheva et al. 2010, Villalta et al. 2013), **128** was designed as a highly specific inhibitor of the trypanosomal enzyme by introducing additional aromatic interactions between the protein and the ligand in the depth of the CYP51 binding cavity (see Figures 44 and 45). **128** displayed an improved anti-parasitic activity (EC_{50} against *T. cruzi* amastigotes from infected cardiomyocytes 0.8 nM for **128** vs. 1.3 nM for **127**), cures experimental Chagas disease with 100% efficiency, is orally bioavailable and has low off-target activity as well as favorable pharmacokinetics.

Not only crystallography but also docking studies were employed in the design of CYP51 inhibitors. More recently, docking of imidazoles (De Vita et al. 2016) and pyrazolo[3,4-e][1,4]thiazepin-based inhibitors (Ferreira de Almeida Fuiza et al. 2018) against TcCYP51 crystal structures identified this enzyme as a potential target, which rationalized the observed anti-*T. cruzi* activities of the compounds.

An interesting complement to the efforts guided solely by static crystal structures are molecular dynamics (MD) simulations, performed by Yu et al. (2015, 2016), used to study ligand egress routes in

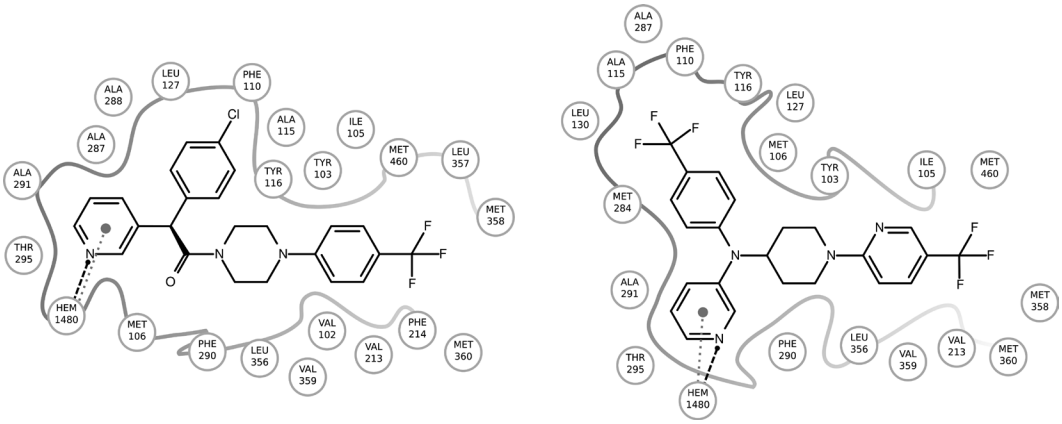

Figure 43. Interaction diagrams of two pyridine-based inhibitors of TcCYP51, **125** and **126**. The diagrams are based on the crystallographic complexes with PDB-ID 3zg2 and 3zg3 (Hargrove et al. 2013), respectively. Pocket-lining residues and the pocket shape are shown. Black dashed lines indicate coordination bonds between the ferric heme iron and a nitrogen atom of the ligand and gray dotted lines indicate π-π interactions.

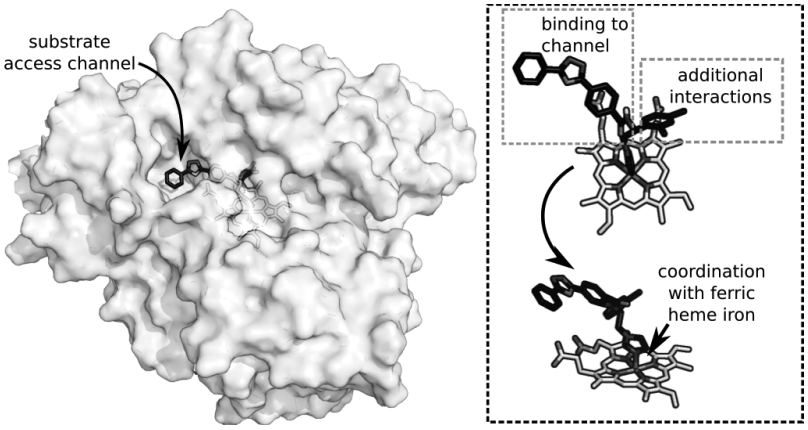

Figure 44. Compound **127** binding to TcCYP51 (see also Figure 42, based on PDB-ID 3gw9; Lepesheva et al. 2010), occupying the substrate access channel and coordinating with the ferric heme iron. The protein is shown as a semi-transparent surface with the ligand in black and the heme group in white sticks. The channel opening towards the surface is marked. On the right side, the protein was removed for clarity. One part of the ligand binds to the channel, while a second portion forms additional interactions in the depth of the pocket. The top view was rotated by approx. 45° to show the coordination between the ligand and the ferric heme iron in the lower panel.

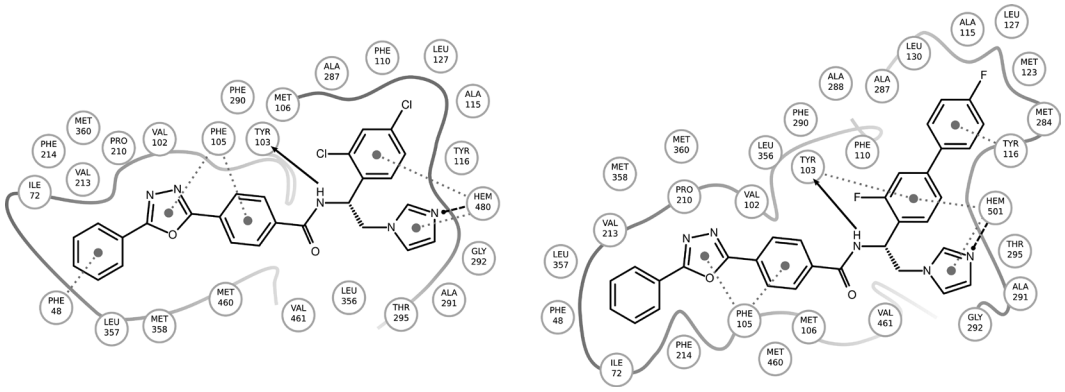

Figure 45. Interaction diagrams of two inhibitors of *Tb*CYP51, **127** and its optimized derivative **128**. The diagrams are based on the crystallographic complexes with PDB-ID 3gw9 and 4g7g (Lepesheva et al. 2010, 2015), respectively. Pocket-lining residues and the pocket shape are shown. Black dashed lines indicate coordination bonds between ferric heme iron and a nitrogen atom of the ligand, gray dotted lines with filled circles indicate π-π interactions, gray dotted lines with white circles cation-π interactions and black arrows show hydrogen-bonding interactions.

T. brucei CYP51 in comparison with human CYP51. These studies highlight differences in the dynamics and composition of the ligand tunnel between the trypanosomal and human CYP51, which could be exploited in the future anti-parasitic drug design efforts to enhance selectivity.

Gunatilleke et al. (2012) combined target-based high-throughput screening (HTS) with a screen against *T. cruzi*-infected skeletal myoblast cells to yield compounds with a known molecular target and activity against the parasite. Further, they used bioinformatics approaches to demonstrate similarities between compounds preferentially bound by CYP51 and compounds bound by several other cytochrome P450 enzymes and an unrelated glutaminyl-peptide cyclotransferase. Inhibitors of these enzymes can hence serve as a potential pool of lead compounds.

It is not uncommon that large libraries of potential hit compounds are screened *in silico* against large crystallographic databases of enzymatic targets. A drawback of such screens is that many studies lack experimental validation of their results. Nevertheless, *in silico* studies exploring, for example, potential

targets of phytochemicals may provide some first insight when a target is not known or may be used to propose possible hits for a desired target. For example, compounds isolated from Nigerian medicinal plants have been studied by Setzer and Ogungbe (2012). They found *in silico* potential inhibitors of, amongst others, TbCYP51 and two enzymes of the parasitic folate pathway: pteridine reductase 1 (PTR1) and dihydrofolate reductase (DHFR).

Further details on the current structural knowledge about CYP51 in trypanosomatids and the design of inhibitory compounds can be found in the recent review by Lepesheva et al. (2018).

Folate metabolism

Targeting the kinetoplastid folate pathway, unlike the corresponding malarial (Hawser et al. 2006) and bacterial (Yuthavong et al. 2005) pathways, requires not only the inhibition of dihydrofolate reductase (DHFR), but also of pteridine reductase 1 (PTR1) (Bello et al. 1994, Sienkiewicz et al. 2010). The latter enzyme is mainly responsible for the reduction of pterins, but can be upregulated when DHFR is inhibited and serve as a bypass for folate reduction to provide necessary educts for DNA synthesis and thus ensure parasite survival (Dawson et al. 2006, Vickers and Beverley 2011). In *T. brucei*, PTR1 was validated as a potential drug target by the gene knockout and RNA interference experiments (Ong et al. 2011, Sienkiewicz et al. 2010). Herein, we mostly focus on inhibitor design for PTR1 from *T. cruzi* and *T. brucei*. Multiple drug design approaches have been used to target PTR1, starting from optimization of the substrate scaffold, through virtual screening (VS), to fragment-based drug design (FBDD).

An example of a classical substrate-like compound is methotrexate **129** (MTX), which is a subnanomolar inhibitor of DHFR, and an approved anti-cancer drug (Zuccotto et al. 1999, Shuvalov et al. 2017). However, it has also been shown to inhibit PTR1 at the sub-micromolar level (Dawson et al. 2006, Cavazzuti et al. 2008). Notably, the substrate, MTX and most other inhibitors of PTR1 occupy the main binding site in a π-sandwich between the nicotinamide of the NADPH/$NADP^+$ cofactor and a phenylalanine residue (Figure 46). MTX adopts a similar binding mode to folate **130**, but with a flipped orientation of the pteridine ring (Figure 46).

The aformentioned binding modes of folate and MTX were starting points in the study by Tulloch et al. (2010), who selected 3 scaffolds—pteridine, pyrrolopyrimidine and pyrimidine—for inhibitor design and optimization against *T. brucei* PTR1 (TbPTR1). Five pyrrolopyrimidine-based inhibitors were identified and crystallized in TbPTR1. Among those, **131** and **132** (Figure 47) with K_i values against TbPTR1 of 0.36 μM and 0.40 μM, respectively, were found to attain modest ED_{50} values against the *T. brucei* bloodstream form (BSF): 274 ± 7.5 μM and 123 ± 3.3 μM, respectively. **132** was also found to show a synergistic effect when combined with MTX. Later, Khalaf et al. (2014) used a similar approach for the development of 61 additional pyrrolopyrimidines, of which 23 were crystallized in TbPTR1, greatly expanding the structural data available for this enzyme. Two of the crystallized compounds, **133** and **134** (Figure 48), had TbPTR1 K_i^{app} values of 0.23 μM and 0.14 μM, respectively, and were found to have *T. brucei* BSF IC_{50} values of 3.20 μM and 0.25 μM, respectively, in Creek's minimal medium. However, these derivatives showed substantial toxicity in *in vivo* mouse models and thus were not suitable for further development.

VS approaches were used to identify novel non-pteridine scaffolds, including the 2-aminothiadiazole core and flavonoids as potential binders of the PTR1 substrate pocket (Ferrari et al. 2011, Borsari et al. 2016). Recently, a library of 2-aminothiadiazole-based TbPTR1 inhibitors has been developed (Linciano et al. 2017). X-ray crystallography and docking simulations confirmed the classical binding mode for these series (cf. Figure 46), with the amino moiety of the scaffold core interacting with a serine residue close to the active site, cofactor ribose and phosphates (Figure 49). Two thiadiazole-2,5-diamines **136** and **137** (Figure 49) reached TbPTR1 IC_{50} values of 16.0 μM and 25.0 μM, respectively. Despite being unable to inhibit the *T. brucei* BSF as single agents, both PTR1 inhibitors potentiated the EC_{50} of MTX by 4.1 and 2-fold, respectively.

Another class of hits against PTR1 were flavonoids, identified by computational and experimental screening of a natural products library (Borsari et al. 2016), with flavonols showing the most promising inhibitory effect on TbPTR1. A combination of crystallographic experiments and computational docking

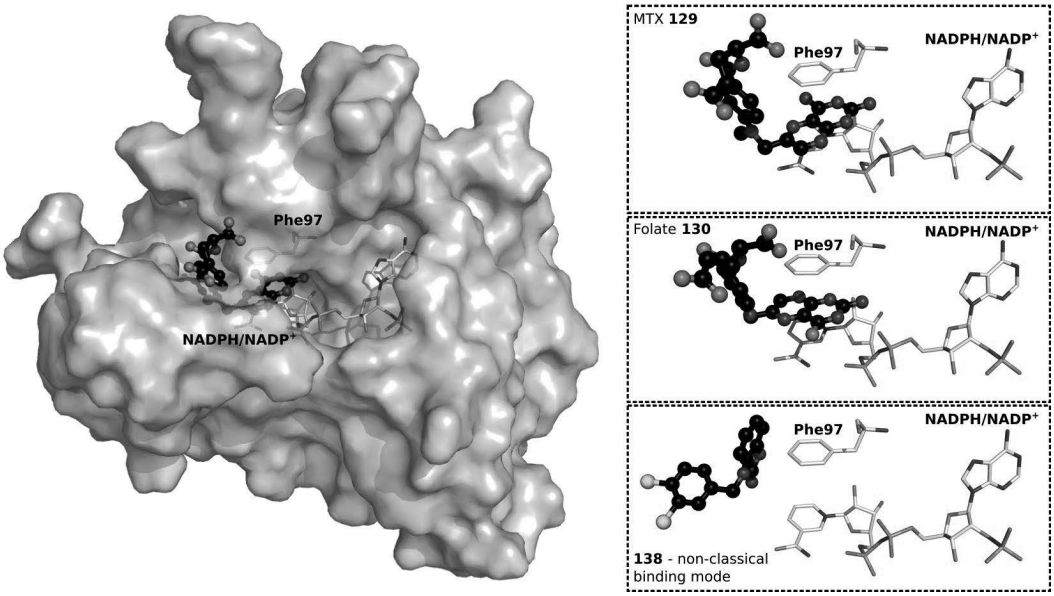

Figure 46. Illustration of compounds binding in the π-sandwich between Phe97 and the nicotinamide of the NADPH/NADP+ cofactor of *Tb*PTR1. On the left, a monomer of the homotetrameric enzyme is shown as a semi-transparent surface representation with bound MTX **129** in dark ball-and-stick representation and the cofactor and Phe97 in white sticks. In the right-hand panel, the same representation is used, omitting only the protein. The complex with MTX **129** is based on PDB-ID 2c7v (Dawson et al. 2006), with folate **130**—on PDB-ID 3bmc (Tulloch et al. 2010) and with **138**, illustrating the non-classical binding mode outside the π-sandwich—on PDB-ID 3gn2 (Mpamhanga et al. 2009).

Color version at the end of the book

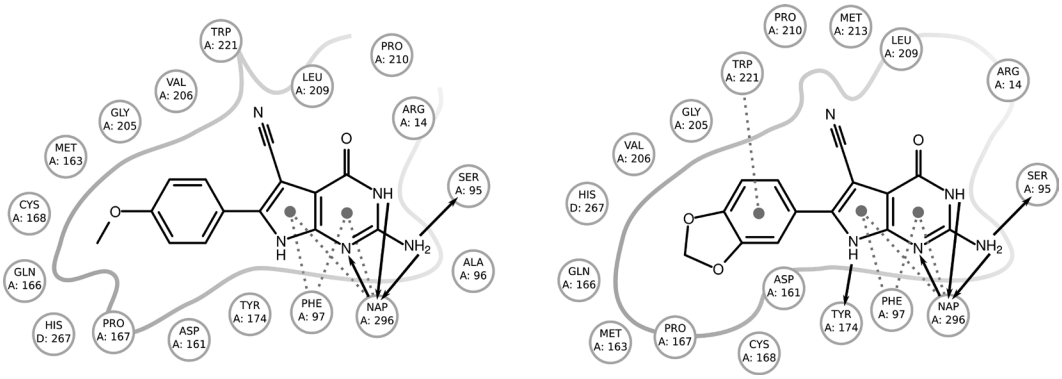

Figure 47. Interaction diagrams of two pyrrolopyrimidine-based inhibitors of *Tb*PTR1, 131 and 132. The diagrams are based on the crystallographic complexes with PDB-ID 3jqe and 3jq9 (Tulloch et al. 2010), respectively. Pocket-lining residues and the pocket shape are shown. Gray dotted lines indicate π-π interactions and black arrows show hydrogen-bonding interactions. NAP denotes NADP(H).

was then employed to explore the multiple possible binding modes and deduce a structure-activity relationship (SAR) for a set of synthetic flavonols. In a follow-up project, the same methods allowed in-depth characterization of the determinants of the activities of several flavonols and the corresponding flavanones (Di Pisa et al. 2017).

In another VS study, Dube et al. (2014) used a combination of docking and pharmacophore modeling to screen the ZINC database for putative inhibitors of TbPTR1 and predict their activities. The VS of

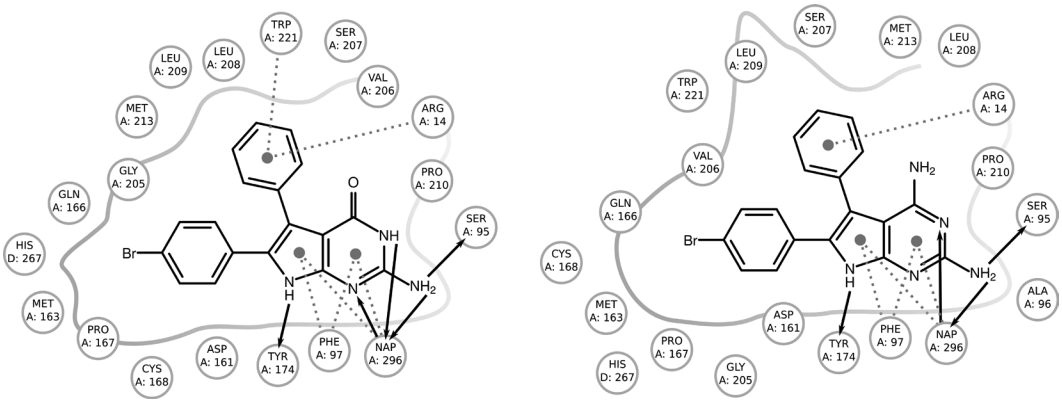

Figure 48. Interaction diagrams of two additional pyrrolopyrimidine-based inhibitors of *Tb*PTR1, **133** and **134**. The diagrams are based on the crystallographic complexes with PDB-ID 4cmi and 4cmj (Khalaf et al. 2014), respectively. Pocket-lining residues and the pocket shape are shown. Gray dotted lines indicate π-π interactions and black arrows show hydrogen-bonding interactions. NAP denotes NADP(H).

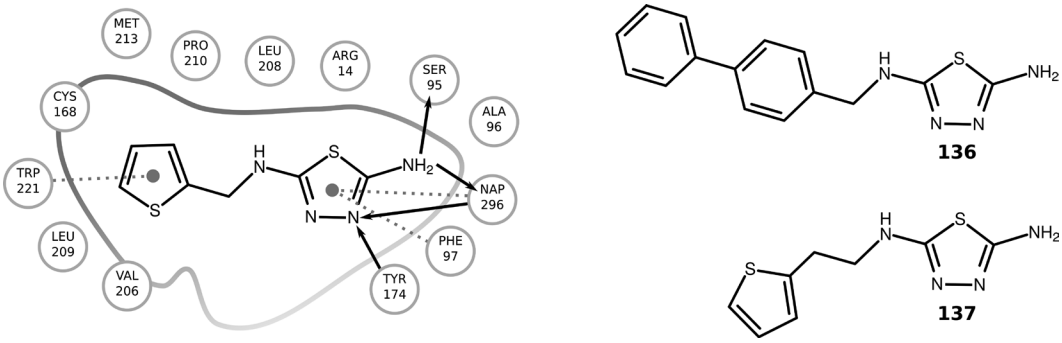

Figure 49. Interaction diagrams of a 2,5-diamino-1,3,4-thiadiazole inhibitor of *Tb*PTR1, **135** and structures of its derivatives **136** and **137**. Compounds **136** and **137** were predicted to show a similar binding mode in *Tb*PTR1 by docking studies (Linciano et al. 2017). The interaction diagram is based on the crystallographic complex with PDB-ID 5izc. Pocket-lining residues and the pocket shape are shown. Gray dotted lines indicate π-π interactions and black arrows show hydrogen-bonding interactions. NAP denotes NADP(H).

fragments against TbPTR1 performed by Mpamhanga et al. (2009) identified 2-aminobenzothiazole and 2-aminobenzimidazole, binding in the substrate pocket, as promising cores that were further used for inhibitor development. Notably, the crystallographic studies revealed that some of the synthesized compounds with a 2-aminobenzimidazole scaffold adopted a non-classical binding mode in the TbPTR1-specific subsite adjacent to the primary substrate binding site (Mpamhanga et al. 2009; Figure 46, compound **138**). Compounds **138** and **139** (Figure 50) reached K_i^{app} of 0.4 μM and 0.007 μM, respectively, against TbPTR1. Despite its nanomolar on-target potency, **138** displayed an EC_{50} against *T. brucei* of only 10 μM. Spinks et al. (2011) further attempted to optimize the series of 2-aminobenzimidazoles to target the alternative subsite, but anti-parasite activities did not improve, with the lowest EC_{50} value being 6.7 μM.

The non-classical binding mode of the amino-benzimidazole series discussed above inspired computational FBDD studies to combine a scaffold with a classical binding mode with an alternative subpocket-targeting scaffold. In principle, computational methods exist that may help in finding the best molecular fragment binding the subsite. However, in the case of the *Tb*PTR1 alternative subsite exploited by Mpamhanga et al. (2009) and Spinks et al. (2011), this was challenging due to the presence of halogen substituents in the most potent compounds. Many state-of-the-art commonly used force fields used in

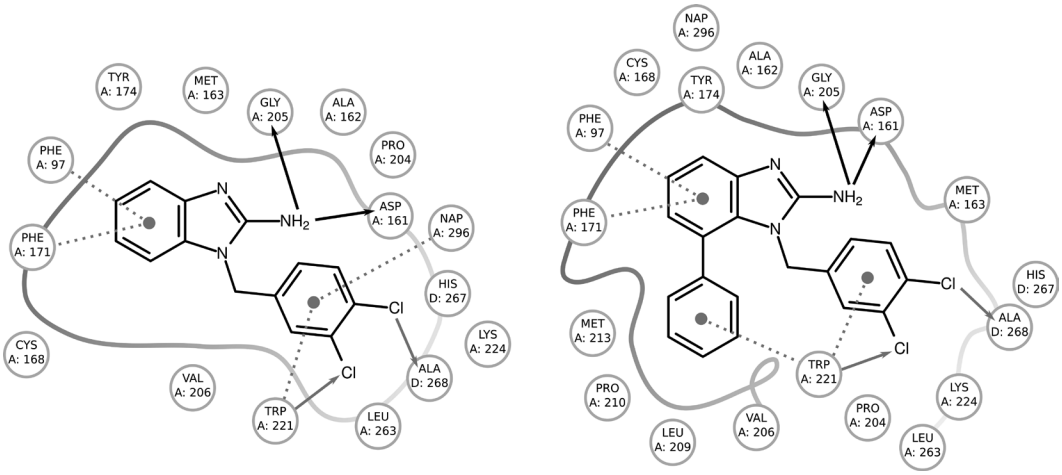

Figure 50. Interaction diagrams of two 2-aminobenzimidazole-based inhibitors of *Tb*PTR1 binding in a non-classical binding mode, **138** and **139** (cf. also Figure 46). The diagrams are based on the crystallographic complexes with PDB-ID 3gn2 and 2wd8 (Mpamhanga et al. 2009), respectively. Pocket-lining residues and the pocket shape are shown. Gray dotted lines indicate π-π interactions, black arrows show hydrogen-bonding interactions and gray arrows indicate halogen-bonds.

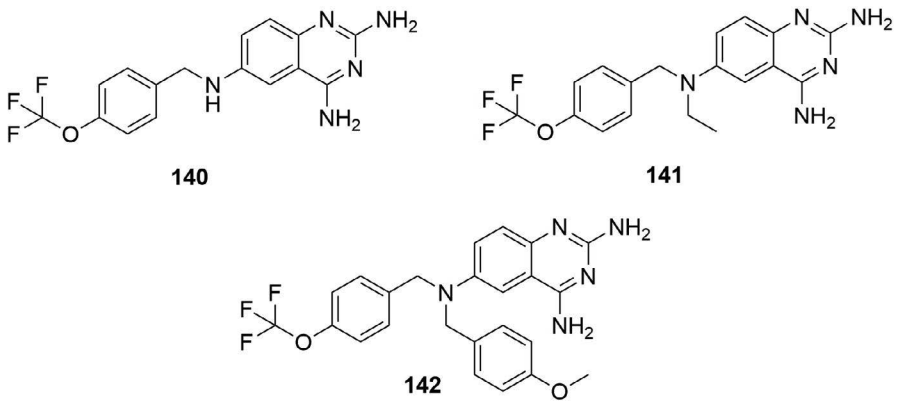

Figure 51. Structures of the quinazoline derivatives **140–142** that putatively target TcPTR2/TcDHFR.

molecular docking suffer from short-comings in the representation of halogens (Wilcken et al. 2013). Thus, using the 2-aminobenzimidazole series by Mpamhanga et al. (2009) and Spinks et al. (2011), Jedwabny et al. (2017) demonstrated how a computationally efficient quantum-mechanics-based model for predicting binding affinities of fragments in the *Tb*PTR1 binding site could be used to overcome these issues.

The majority of compounds have been developed to target *Tb*PTR1 (or *Leishmania major* PTR1). Although a crystal structure of a close homolog of *Tc*PTR1, *Tc*PTR2, was solved (Schormann et al. 2005), most drug design efforts did not consider the *T. cruzi* enzyme variants. Mendoza-Martínez et al. (2015) designed some quinazoline derivatives and used docking studies to support TcPTR2 and TcDHFR as reasonable potential targets. The compounds were evaluated against bloodstream trypomastigotes of two strains of *T. cruzi* (NINOA and INC-5 strain) and compounds **140–142** (Figure 51) were found to be particularly interesting, since they showed a better activity profile than the reference drugs, nifurtimox and benznidazole.

Otherwise, for *T. cruzi*, mainly DHFR was considered in drug design efforts: Schormann et al. (2008) used 3D-QSAR models to guide the design of inhibitors selective for TcDHFR over human DHFR (hDHFR). In the subsequent study, guided by crystallography and docking experiments, they exploited amino acid

differences between the pocket entrance regions of hDHFR and TcDHFR, including the substitution of Phe31 to Met49. A series of 2,4-diaminoquinazoline derivatives, similar to trimetrexate, with varying flexible hydrophobic groups in the tail, some of which bound near Met49 of TcDHFR, had about 7–8 times better K_i against TcDHFR than hDHFR (Schormann et al. 2010).

The above discussed study of Mendoza-Martínez et al. (2015) is an example of a dual inhibition approach, which is particularly important for targeting the trypanosomatid folate pathway. Ideally, this requires targeting both PTR1 and parasitic DHFR, while avoiding inhibitor binding to hDHFR, which is quite similar to the parasitic homologue. To address this issue, Panecka-Hofman et al. (2017) applied a variety of techniques (such as computational analysis of crystallographic structures, homology modeling and binding site mapping) for sequence and structural comparison of the folate pathway on- and off-targets. Ligand-target interactions, binding site properties and target conformational variability were computationally compared to yield guidelines for the design and optimization of selective inhibitors of the trypanosomatidic folate pathway. In an extension of this study, the conformational variability of the TcDHFR and hDHFR binding sites was analyzed with the TRAPP (TRAnsient Pockets in Proteins) web server based on the available crystallographic data (Stank et al. 2017). Complementary to the aforementioned work of Schormann et al. (2010), a transiently appearing subpocket was identified in the vicinity of Met49, which corresponds to Phe31 in hDHFR. The ProSAT+ tool integrated in TRAPP also identified position 31 as a known site of an hDHFR mutation that alters binding of the MTX inhibitor.

The majority of drug design efforts for the kinetoplastid folate pathway have so far focused on PTR1/PTR2 and DHFR. A few other folate pathway enzymes, such as the N^5,N^{10}-methylenetetrahydrofolate dehydrogenase/cyclohydrolase (DHCH) of *T. brucei*, were considered in compound development. Eadsforth et al. (2015) designed inhibitors of TbDHCH using a combination of crystallographic and docking experiments starting from an inhibitor of bacterial and human DHCH.

Despite the extensive design and development efforts to obtain potent and selective inhibitors of PTR1 and DHFR, there is often limited transferability of on-target-based activity to an *in vitro* or even *in vivo* activity against *T. brucei* or *T. cruzi*. For a more detailed overview on the efforts made, possible reasons for this limitation and other potential targets to be considered in the future, the reader is referred to the recent review by Cullia et al. (2018).

Phosphodiesterases

More recently, a phosphodiesterase (PDE) of *T. brucei*, the PDEB1 isoform, has gained attention as a potential drug target for Human African Trypanosomiasis (HAT). Phosphodiesterases cleave phosphodiester bonds in cyclic nucleotides like cyclic AMP (cAMP), which is an important second messenger involved in regulation of signal transduction. An overview about cAMP signalling in trypanosomatids and differences between parasitic and human pathways that can be exploited for drug discovery can be found in the review by Tagoe et al. (2015). Herein, we focus on the recent efforts made to develop inhibitors of *Tb*PDEB1.

Since inhibitors of human PDEs, like cilomilast, piclamilast, sildenafil and tadalafil were known, design efforts were often focused on repurposing these drugs and developing analogs thereof (Amata et al. 2014, Ochiana et al. 2012, Wang et al. 2012, Woodring et al. 2013), but with rather limited success. For example, Amata et al. (2014) found that cilomilast **143** (Figure 52) had an IC_{50} of 16.4 μM against *Tb*PDEB1 and the best derivative **144** (Figure 52) resulted in an IC_{50} of 0.95 μM. However, the EC_{50} of **144** in a cellular assay against *T. brucei* was still only modest (26 μM vs. cilomilast **143** $EC_{50} > 50$ μM).

A virtual screening of the ZINC database was carried out by Jansen et al. (2013) to broaden the chemical space of the potential TbPDEB1 inhibitors. Molecular docking in conjunction with a score based on receptor-compound interaction fingerprints was used to filter suitable compounds. This way, six novel inhibitors of TbPDEB1 with IC_{50} values between 10 and 80 μM were identified.

In another study, Orrling et al. (2012) used homology modeling and docking studies to exploit a parasite-specific subpocket, the so-called P-pocket of TbPDEB1 (Figure 53), for the design of the improved catechol pyrazolinone-based inhibitors. The most potent inhibitor **145** (Figure 54) achieved an IC_{50} of 49 nM against TbPDEB1 and was able to inhibit parasite trypomastigote proliferation in *in vitro* studies: *T. brucei rhodesiense* with IC_{50} of 60 nM, *T. brucei brucei* with IC_{50} of 520 nM and *T. cruzi* with IC_{50} of

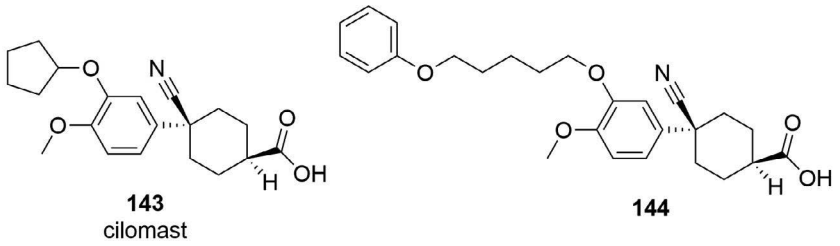

Figure 52. Structures of the human PDE inhibitor cilomilast **143** and its derivative **144** optimized for *Tb*PDEB1 targeting.

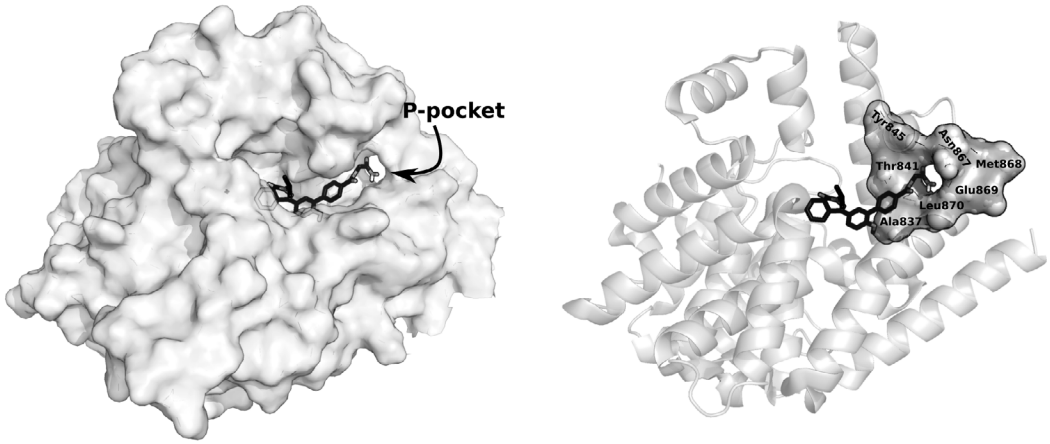

Figure 53. Compound **147** binding to *Tb*PDEB1 (see also Figure 52, based on PDB-ID 5l8c) and targeting the parasite PDE-specific P-pocket. On the left, the protein is shown as a semi-transparent surface with the ligand in black sticks and the location of the P-pocket marked. On the right side, the protein is shown in the same orientation as cartoon and only the P-pocket residues are shown as a surface with residues labeled according to Blaazer et al. (2018).

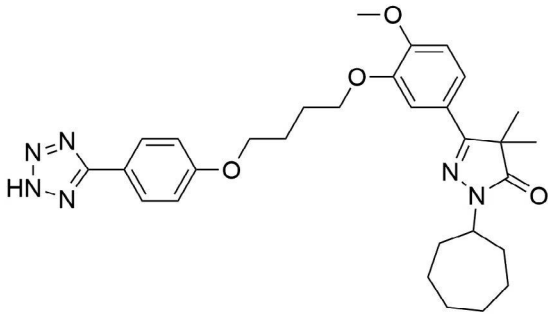

Figure 54. Structure of the P-pocket targeting *Tb*PDEB1 inhibitor **145**.

7.6 μM. However, compound **145** was an even more potent inhibitor of human PDE isoforms. Thus, this study highlights the potential of PDE inhibitors against trypanosomal infections, but also indicates that further optimization of the selectivity for the TbPDEB1 target is required.

The P-pocket of TbPDEB1 has been recently further exploited by Blaazer et al. (2018) in their development of selective 4a,5,8,8a-tetrahydrophthalazinone-based inhibitors. Guided by the crystallographic analysis of non-specific TbPDEB1 inhibitors and the analysis of flexibility patterns of a TbPDEB1-inhibitor complex observed by MD simulations, several compounds specifically targeting the P-pocket were developed. **146** and **147** (Figure 55) were overall the best, both showing K_i of 100 nM

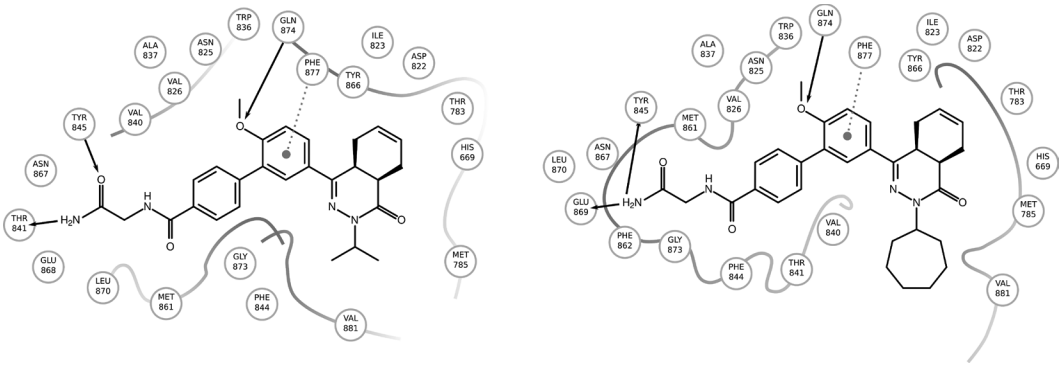

Figure 55. Interaction diagrams of the two P-pocket-targeting *Tb*PDEB1 inhibitors, **146** and **147** (cf. Figure 53). The diagrams are based on the crystallographic complexes with PDB-ID 5g2b and 5l8c (Blaazer et al. 2018), respectively. Pocket-lining residues and the pocket shape are shown. Gray dotted lines indicate π-π interactions and black arrows show hydrogen-bonding interactions.

against TbPDEB1, 10- and 19-fold selectivity for the parasitic over the human enzyme, and had IC_{50}s of 5.5 μM and 6.7 μM, respectively, when tested against *T. brucei*.

Cysteine proteases

Two cysteine proteases structurally related to human cathepsin, L: cruzain of *T. cruzi* and rhodesain of *T. brucei rhodesiense*, have been subject to many drug development efforts, including many computational and mechanistic studies in the past years, which we review below. More details on inhibitor design against cysteine proteases in *Trypanosoma* can be found in the recent review by Ferreira and Andricopulo (2017).

Cruzain: Since cruzain is a protease, many inhibitors designed were based on peptides and typically bind covalently (see Figure 56). Database screening strategies led to non-peptide inhibitors of cruzain. Ferreira et al. (2010) illustrated for cruzain inhibitors how the combination of VS, HTS and prioritization of molecular scaffolds can largely avoid false-positives. Wiggers et al. (2013) identified non-covalent cruzain inhibitors from the ZINC database. Further, Palos et al. (2017) performed VS of FDA-approved drugs against cruzain and confirmed the trypanocidal potential of four putative inhibitors *in vitro* and *in vivo*, which may thus represent starting scaffolds for further drug development.

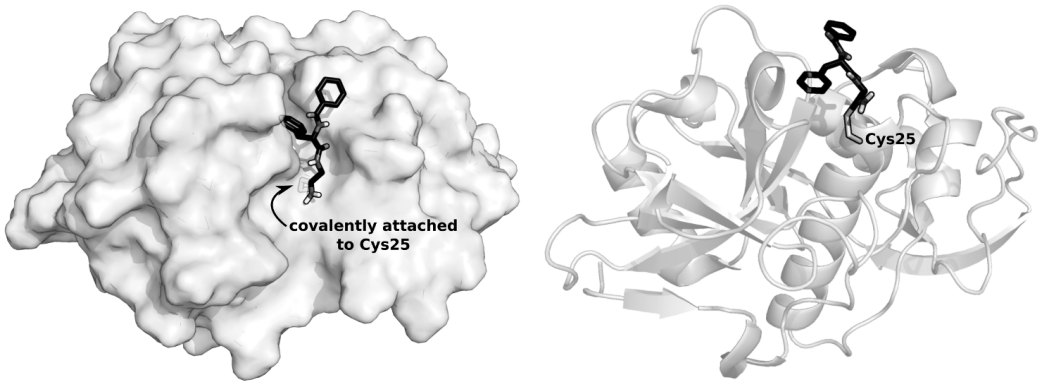

Figure 56. Example of a dipeptidyl nitrile ligand **148** covalently attached to the cysteine protease cruzain (see also Figure 57, based on PDB-ID 4qh6; Avelar et al. 2015). On the left, the protein is shown as a semi-transparent surface with the ligand in black sticks. On the right, the protein is shown in cartoon representation, rotated by about 90° and the site of the covalent attachment, Cys25 is labeled.

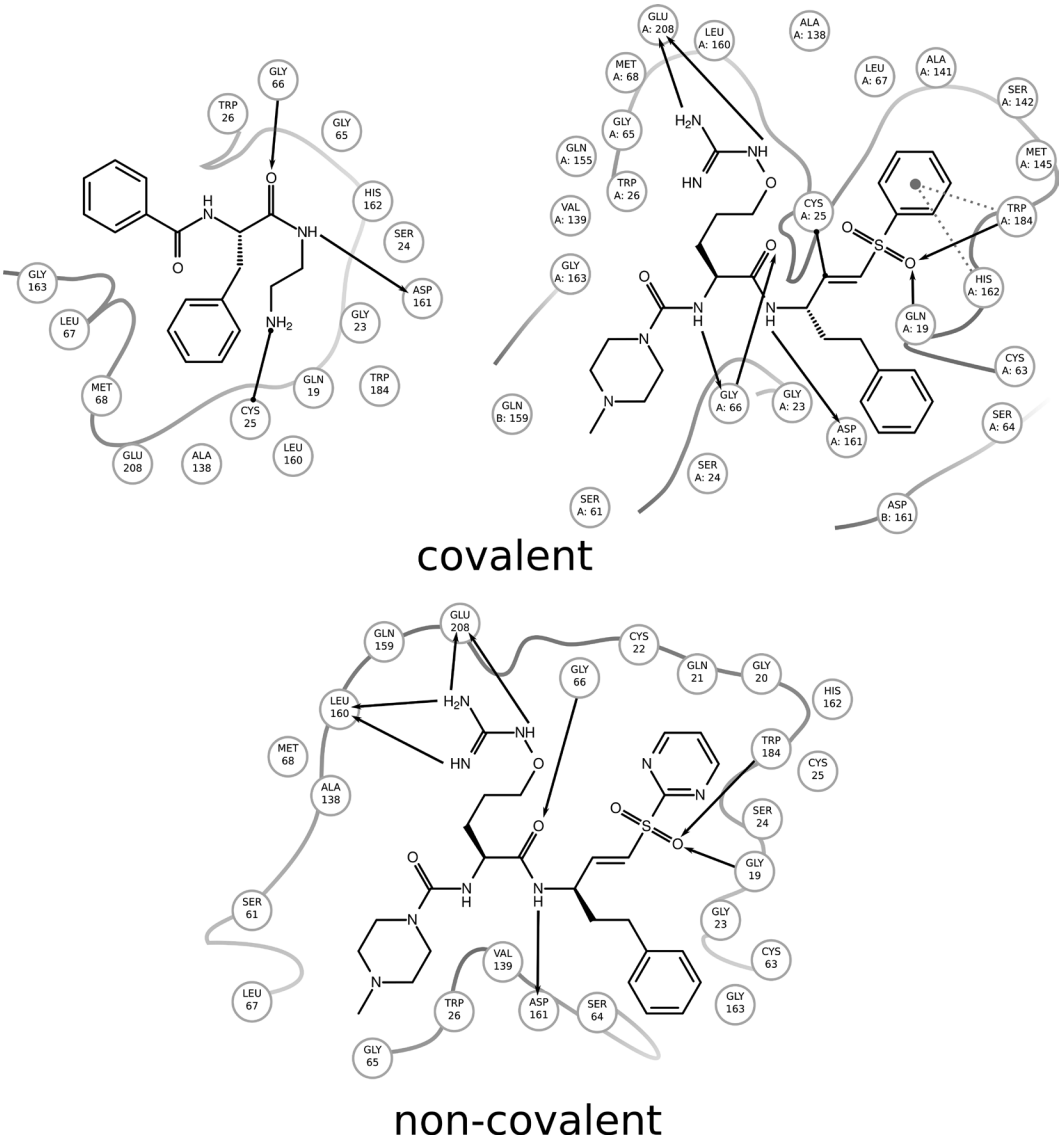

Figure 57. Interaction diagrams of cruzain inhibitors: the covalent dipeptidyl nitrile **148** (left, see also Figure 56; Avelar et al. 2015) and non-covalent oxyguanidine inhibitors **149** and **150** (middle and right; Jones et al. 2015). The diagrams are based on the crystallographic complexes with PDB-ID 4qh6, 4pi3 and 4xui, respectively. Pocket-lining residues and the pocket shape are shown. Gray dotted lines indicate π-π interactions, black arrows show hydrogen-bonding interactions, and a black line ended with circles marks a covalent bond between ligand and protein.

Crystallography was also used for exploring compound binding modes, MoA, and for obtaining SAR. In the aforementioned VS study, Wiggers et al. (2013) used a molecular simplification approach to obtain a SAR for one of the compounds and found that the 2-acetamidothiophene-3-carboxamide scaffold was the critical component for the interactions with cruzain. Then, they confirmed the binding mode of this scaffold by crystallographic data, thus validating a potential new non-covalent, non-peptidic cruzain-binding scaffold. Avelar et al. (2015) characterized dipeptidyl nitriles as inhibitors of cruzain by extensive SAR studies and determining a crystallographic complex with compound **148** (Figures 56 and 57). Jones et al. (2015) synthesized and crystallized oxyguanidine analogs of existing cysteine protease inhibitors

and were able to show that one of the compounds displays covalent (**149**, Figure 57) and the other non-covalent inhibition (**150**, Figure 57).

A variety of computational chemistry methods has been used to study cruzain interactions with inhibitors, to better understand their MoA, and to design new compounds. Hologram quantitative structure-activity relationship, comparative molecular field analysis and comparative molecular similarity index analysis methods combined with docking simulations have been applied to a series of benzimidazole-based cruzain inhibitors by Pauli et al. (2017) to predict binding modes and activities. Silva et al. (2017) used docking studies and QSAR methods to study nitrile-containing cruzain inhibitors and predict their activities, leading to the proposal of new potential inhibitors. de Souza et al. (2017) used 2D- and 3D-QSAR methods to explore the interactions of oxadiazole-based compounds with different cruzain subsites. Elizondo-Jimenez et al. (2017) synthesized benzenesulfonyl and N-propionyl benzenesulfonyl hydrazone derivatives, evaluated their anti-*T. cruzi* activity and used docking studies to propose covalent binding to cruzain as the compounds' MoA. Silva-Júnior et al. (2016) synthesized several trypanocidal thiophen-2-iminothiazolidines and used molecular docking to demonstrate that the most active compound likely interacts simultaneously with two subsites of cruzain.

To gain more insight into cruzain dynamics and its interactions with inhibitors, MD simulations have been applied together with other molecular modelling techniques. Durrant et al. (2010) used sequence analysis and MD simulations to explore additional binding sites in cruzain. Hoelz et al. (2016) studied free and liganded cruzain dynamics at acidic pH, which corresponds to its environment in the cell. Very recently, Cianni et al. (2018) also used MD simulations to study the binding mode of reversible covalent inhibitors to the less frequently studied specific subsite S3 of cruzain. Finally, Martins et al. (2018) demonstrated a comprehensive computational approach including docking, MD, *ab initio* and MM/PBSA calculations for binding mode prediction and estimation of the contributions of specific amino acids to binding. Finally, more mechanistic approaches have been carried out, for example by Arafet et al. (2015, 2017) who studied the MoA of peptidyl-epoxyketone- or peptidyl-halomethyl-ketone-based cruzain inhibitors with a QM/MM method.

Rhodesain: For rhodesain, several SBDD efforts were inspired by its structural similarity to human cathepsin. Triazine nitrile-based compounds were studied against rhodesain and extensive SAR analyses were performed to explore the binding preferences of the different subsites, supported by a crystallographic complex of the synthesized compounds with the structurally related human cathepsin L enzyme (Ehmke et al. 2013). Schirmeister et al. (2017) aimed at repurposing human cathepsin-targeting dipeptide nitriles for rhodesain and used covalent docking to support the development of a SAR. Later, Giroud et al. (2018) optimized a set of macrocyclic lactams, developed as human cathepsin L inhibitors, to target *T. brucei* rhodesain and elucidated their binding modes by crystallographic studies. The initial compound **151** (Figure 58) had a K_i of 11 nM against rhodesain, but also a K_i of 10 nM against human cathepsin L. One of the optimized, designed pyrazole derivatives **152** (Figure 58) was found to be about 11 times more effective as an inhibitor of rhodesain than human cathepsin L (K_i rhodesain 5.2 nM; K_i human cathepsin L 55.7 nM) and to be a potent inhibitor of *T. b. rhodesiense* with an IC_{50} of 0.6 nM.

Trypanothione metabolism

The redox metabolism of parasites like *T. brucei* relies, in contrast to humans, on the dithiol trypanothione **153** (N1,N8-bis(glutathionyl)spermidine; see Figure 59) being absent in humans and making enzymes involved in this pathway interesting as drug targets for trypanosomatidic diseases (Fairlamb and Cerami 1992, Leroux and Krauth-Siegel 2016). One of the best studied and genetically validated targets is trypanothione reductase (TrypR; see Figure 59), which is responsible for reducing trypanothione disulfide (Fairlamb and Cerami 1992, Krieger et al. 2000). In humans, a similar reaction is performed by glutathione reductase, which, however, has an opposite net charge in the active site, facilitating the development of specific inhibitors (Faerman et al. 1996).

Structure-based modelling provided insights into the TrypR pocket regions that could be targeted in drug design approaches. For example, Patterson et al. (2011) designed 3,4-dihydroquinazoline-based

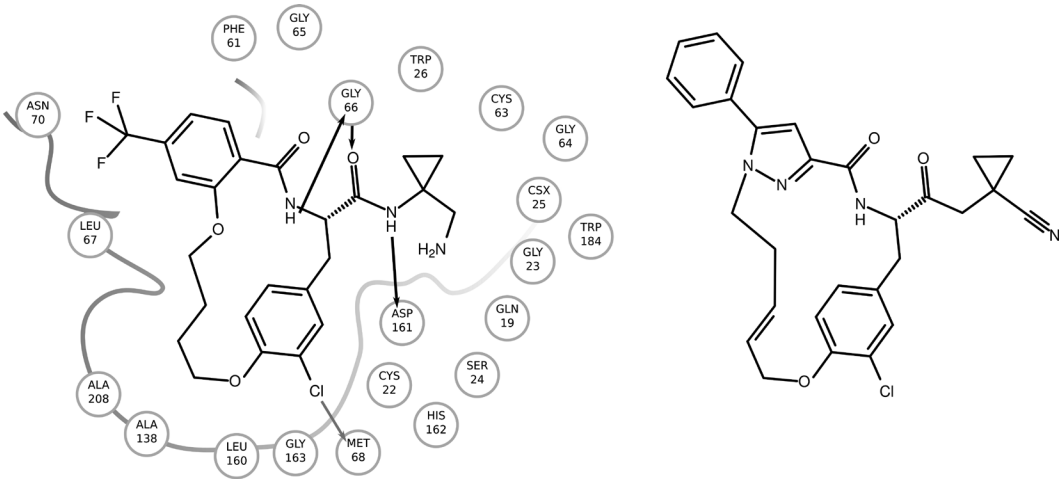

Figure 58. Interaction diagrams of a macrolactam inhibitor of rhodesain **151** (left) and structure of its derivative **152** (right). The interaction diagram is based on the crystallographic complex with PDB-ID 6ex8 (Giroud et al. 2018). Pocket-lining residues and the pocket shape are shown. Black arrows in the interaction diagram indicate hydrogen-bonding interactions.

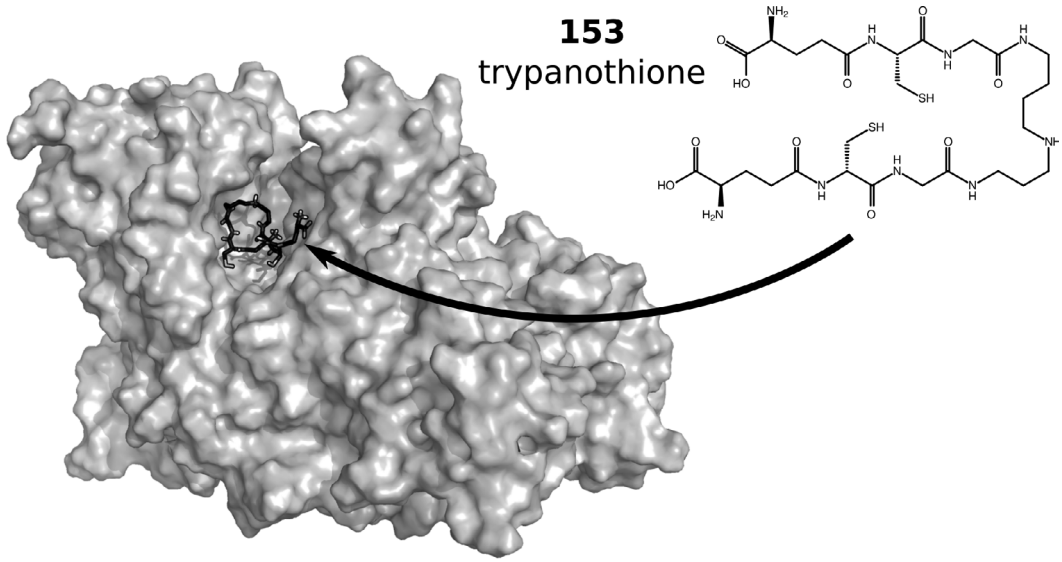

Figure 59. TrypR of *T. brucei* with trypanothione **153** bound at the interface between two chains (based on PDB-ID 2wow, chain A and B, ligand state A; Patterson et al. 2011). The protein is shown as a surface with trypanothione in black sticks.

inhibitors and solved several crystal structures of *T. brucei* TrypR. They observed conformational changes upon ligand binding, initiating the formation of a subpocket, which was exploited in further design and yielded compounds with improved TbTrypR and anti-trypanosomal activity: The initial hit compound **154** (Figure 60) had an IC_{50} of 6.8 µM against TbTrypR and an EC_{50} against *T. brucei* of 40 µM, while the best designed compound **155** (Figure 60) yielded a TbTrypR IC_{50} of 0.23 µM and a *T. brucei* EC_{50} of 0.73 µM.

In a later study, based on a series of peptide-based inhibitors, da Rocha Pita et al. (2012) developed receptor-dependent four-dimensional quantitative structure-activity relationship (RD-4D-QSAR) models (Pan et al. 2003) that allowed for identifying TrypR subsites that may be exploited in future inhibitor development.

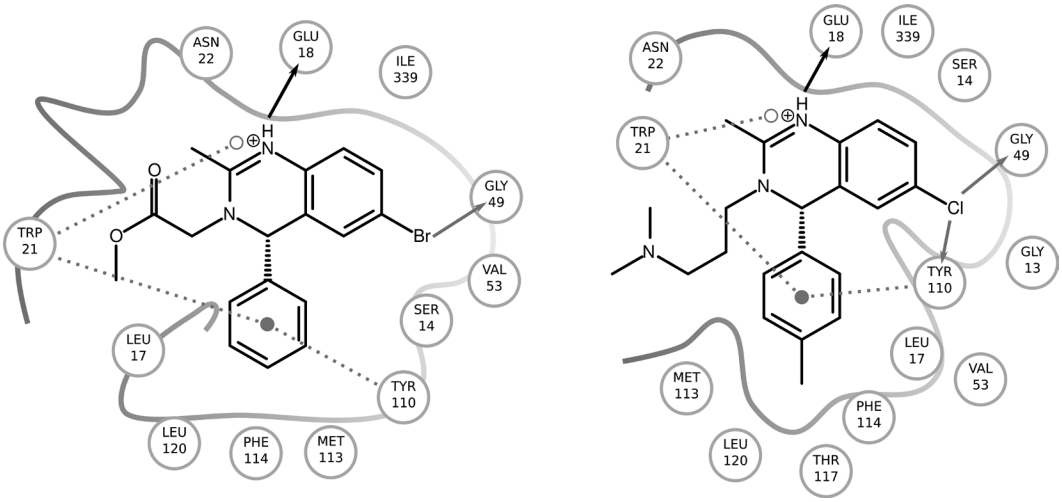

Figure 60. Interaction diagrams of two dihydroquinazoline-based inhibitors of *Tb*TrypR, **154** and **155**. The diagrams are based on the crystallographic complexes with PDB-ID 2wp5 and 2wpf (Patterson et al. 2011), respectively. Pocket-lining residues and the pocket shape are shown. Gray dotted lines indicate π-π interactions, gray arrows indicate halogen-bonding interactions.

Using a combined approach including mutation studies, docking simulations, and crystallography, Persch et al. (2014) developed analogs of 1-[1-(benzo[b]thien-2-yl)cyclohexyl]piperidine as inhibitors of *T. brucei* and *T. cruzi* TrypR, targeting the large substrate binding site (Figure 56). For example, compound **156** (Figure 61) displayed K_i values of 4 ± 0.5 μM against TcTrypR and 12 ± 2 μM against TbTrypR, when assuming a competitive inhibition mechanism. The IC_{50} against *T. cruzi* was 19.0 μM and against *T. brucei rhodesiense*—3.5 μM, with SI of 8 for L6 cells. However, there was some evidence that TrypR might not be the only target of the tested compounds. In a follow-up project (De Gasparo et al. 2018), again with the help of crystallographic studies, the cyclohexylpyrrolidine inhibitors were further optimized by retaining fragments that bind to the hydrophobic substrate binding site and by increasing the polarity of solvent-exposed moieties to improve aqueous solubility.

On the other hand, structure-based techniques helped in identifying TrypR as a potential target for some compounds active at the parasite level. This was the case for propyl/isopropyl quinoxaline-7-carboxylate 1,4-di-N-oxide-based compounds, active against *T. cruzi*, which were found to target TrypR by using docking simulations and enzymatic validation (Chaćon-Vargas et al. 2017). Arias et al. (2017) synthesized a set of nitrofuran derivatives, which demonstrated uncompetitive inhibition of TrypR in subsequent experiments. Docking studies indicated that the inhibitors may in fact be capable of binding to the enzyme-substrate complex, thus explaining the observed behavior. Similar observations were previously made for mesoionic 1,3,4-thiadiazolium-2-aminide (Rodrigues et al. 2012), which was also found to dock to TrypR in the presence of the substrate molecule. Finally, natural products or natural product-derived compounds, such as alkaloids or neolignan derivatives were proposed as inhibitors of TcTrypR on the basis of *in silico* screening, docking studies, and 2D-QSAR analysis (Argüelles et al. 2016, Hartmann et al. 2017).

Other enzymes of the trypanothione pathway were also investigated as potential drug targets. A mathematical model of the *T. cruzi* trypanothione pathway was developed by Olin-Sandoval et al. (2012). The results demonstrated that a polypharmacology approach targeting γ-glutamylcysteine synthetase (γECS) and trypanothione synthetase (TrypS) as the enzymes that exert the highest control on the pathway fluxes may be more promising than targeting TrypR. TrypR was found to have less metabolic control and thus requires very high ligand binding affinities to shut the pathway down. Further, by the same approach, tryparedoxin was identified as a suitable potential drug target, since it shows low catalytic efficiency and exerts large metabolic control (González-Chávez et al. 2015).

In line with the above findings, Benítez et al. (2016) focused on identifying TrypS inhibitors, using target-based screening of a compound library. Furthermore, Vázquez et al. (2017) discovered buthionine

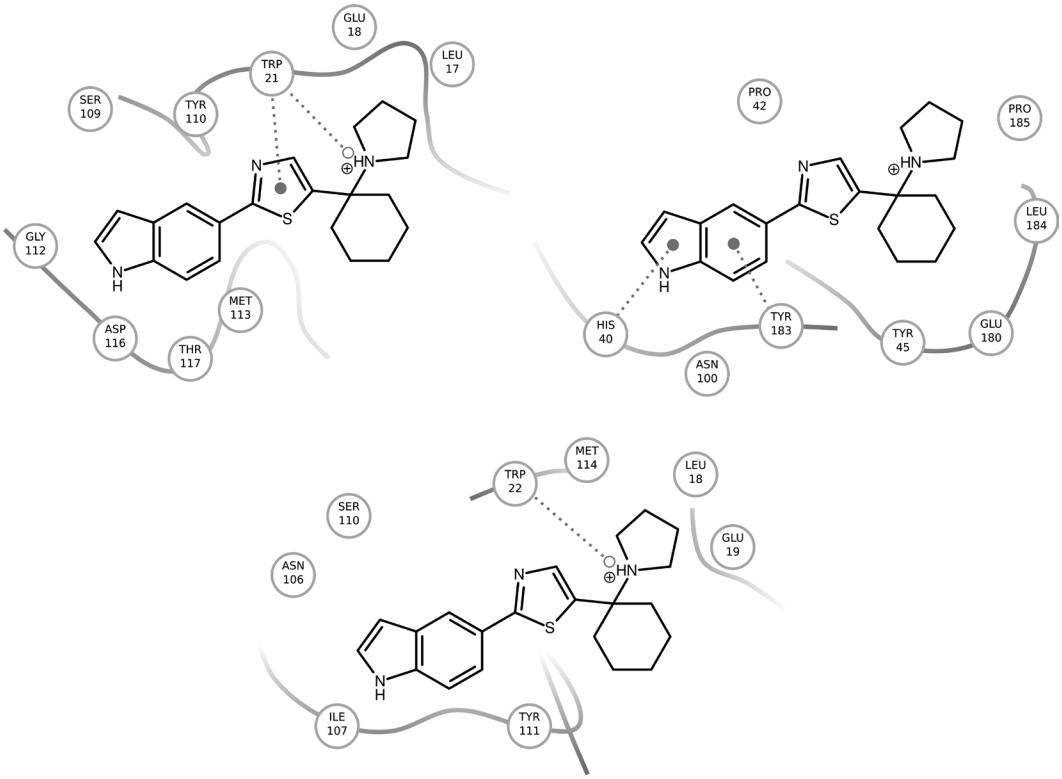

Figure 61. Interaction diagrams of piperidine-based inhibitor **156** in *Tb*TrypR (left) and TcTrypR (right). The diagrams are based on the crystallographic complexes with PDB-ID 4nev and 4new (Persch et al. 2014), respectively. Pocket-lining residues and the pocket shape are shown. Gray dotted lines indicate π-π interactions.

sulfoximine as a dual inhibitor of γECS and TrypS, which was further confirmed by the docking and over-expression experiments.

For a more detailed review on the system and currently known inhibitors of both TrypR and TrypS, the reader is referred to Leroux and Krauth-Siegel (2016).

Perspectives and limitations of target-based drug discovery approaches

Many of the examples presented herein demonstrate that it is not always trivial to translate good activities against a specific biomolecular target into anti-parasitic activity. However, target-guided approaches, like crystallography and computational docking studies, provide important guidelines for scaffold optimization and aid the development of SARs. Further, off-target effects can be minimized by the same techniques and comparative studies of, for instance, sequences, structures and molecular interaction fields. Computational studies of target dynamics provide further hints for desirable flexibility profiles of designed molecules. Moreover, mechanistic insights are gained by studying drug-target interactions. Target-based methods are under continuous development and offer great potential for finding suitable starting points for medicinal chemistry programs and the design of specific, selective compounds with a well-defined MoA. The choice of the target and its impact on the pathway to be inhibited is often a critical bottleneck and mathematical models of trypanosomal metabolic pathways may shed light on which enzymes have most control over pathway fluxes and thus may present the most promising targets. In summary, while many interesting compounds have been developed by target-based design strategies, there are limitations to the approach which are best overcome by combining target-guided approaches with screening of the compounds' anti-parasitic properties early on in the drug discovery process.

In vivo murine models in trypanosomatidic infections

Murine models, due to their small size, availability of tools for genetic manipulation and immunological studies, are at the forefront of animal use in science (Vandamme 2015). Notwithstanding, the use of animals in scientific research has always been a socially polarizing subject even with the implementation of the three Rs (Replacement, Reduction and Refinement) proposed more than 60 years ago (Russell and Burch 1959). For an animal model to be considered, there must be similarities related to disease etiology, pathophysiology, symptomatology and also response to therapeutic or prophylactic agents. In this sense, animal models have contributed decisively to the understanding of pathophysiological processes associated with infection and disease and have also been instrumental in pre-clinical vaccine and drug development.

For HAT, the animal models are well established and have predictive value for drug development (Field, Horn et al. 2017). These models were further solidified using highly susceptible BALB/c mice and bioluminescent parasites that enable longitudinal evaluation of drug performance (McLatchie, Burrell-Saward et al. 2013, Burrell-Saward, Rodgers et al. 2015). Most models that exist are for stage 1 disease using the non-pathogenic *T. b. brucei* S427, although *T. b. rhodesiense* and to a lesser extent *T. b. gambiense* models also exist (Giroud, Ottones et al. 2009, Muchiri, Ndung'u et al. 2015, Field, Horn et al. 2017). Established models for stage 2 are also available using *T. b. brucei GVR35* that induces a slow progressing infection in invasion of the central nervous system (Jennings, Urquhart et al. 1983, Burrell-Saward, Rodgers et al. 2015). For Chagas disease, the situation is quite different, as the translatability of the existing mice models to human disease is not linear as demonstrated by the posaconazole failure (Francisco, Lewis et al. 2015, Molina, Salvador et al. 2015). Many of the standardization issues that affect *Leishmania* mice models are also present in Chagas disease with completely different infection outcomes depending on the parasite strain, stage, inoculum and inoculation route affecting treatment susceptibility (Chatelain and Konar 2015). Like in HAT, there are distinct animal models proposed for acute and chronic stages of the disease. The models for the acute stage are more common in drug development, which normally use high doses of parasites and are expected to be fatal after one month (Romanha, Castro et al. 2010). These models are typically used to demonstrate lack of efficacy of compounds and are considered not to be appropriate for lead development (Chatelain and Konar 2015). Chronic models also exist, requiring several months to be established with disease outcome being highly dependent on the strains used (Marinho, Bucci et al. 2004, Marinho, Nunez-Apaza et al. 2009). Therefore, these chronic models are considered time consuming and are expensive for drug development, requiring in-depth studies of the tissue tropism of the used strains (Chatelain and Konar 2015). A known technical limitation of the Chagas models was, for a long time, the detection of infection. This was problematic as these parasites are often absent from blood, requiring extensive examination of distinct tissues (Field, Horn et al. 2017). Nonetheless, this difficulty has been somewhat minimized with the use of bioluminescent parasites that, in conjunction with immunosuppressive treatments with cyclophosphamide, enable a better assessment of cure (Lewis, Francisco et al. 2015). Consequently, there is the notion that the existing mice models for Chagas disease have a limited predictive value for drug development, raising the need to improve the available mice models for Chagas (Chatelain and Konar 2015, Field, Horn et al. 2017).

Hamsters can be infected with several *Trypanosoma* sp and this species has been considered the most satisfactory and economic animal for maintenance of *T. b. gambiense* infection for experimental studies in laboratories (Lee and Pan 1980). However, as a rule, the use of hamsters as experimental models for HAT has been considerably less relevant compared to mice models (Pink et al. 2005). In the case of *T. cruzi* infections, hamster is considered a valuable model for Chagas disease studies in both acute and chronic phases of the infection (Ramirez et al. 1994), since they reproduce a range of different outcomes of the disease in humans (Bilate et al. 2008).

Ultimately, no perfect animal models exist but they have been essential to advance our knowledge of pathogenic mechanisms involved in these diseases and also to develop successful control approaches through vaccine and drug development (Pasquali 2018).

Au.: Cannot find in refs.

Au.: Cannot find in refs.

Au.: Pl check these.

Au.: Pl check these.

Au.: Pl check these.

Au.: Pl check

Au.: Pl check

Au.: Pl check

Au.: Pl check

Au.: Pl check

Au.: You mean `increasing'?

Au.: Not in refs.

Au.: Not in refs.

Conclusion and Perspectives

In the present chapter, we have highlighted key medicinal chemistry approaches to identifying and assessing new hits and optimizing leads for tackling Chagas disease and HAT. The drug discovery approaches to the identification of new drugs for Chagas disease and HAT take advantage of the scope for collaborative work by different stakeholders, including academic research scientists, national and international organizations and governmental initiatives as well as private research centers and pharmaceutical companies. More financial support for the early stages of research and development is needed. Unfortunately, many research programs start and develop early hits and leads but then fall prematurely into the "valley of death" of unused early and late candidate compounds. A major effort devoted to further developing the most valuable compounds identified should be a core part of future research programs.

Acknowledgements

The Authors acknowledge the European Union's Seventh Framework Programme for research, technological development and demonstration under grant agreement n° 603240 (NMTrypI—New Medicines for Trypanosomatidic Infections). http://www.nmtrypi.eu/JPH acknowledges support from the Polish National Science Centre (grant no. 2016/21/D/NZ1/02806) and the BIOMS program at the Interdisciplinary Center for Scientific Computing IWR, University of Heidelberg.

Abbreviations

BSF	bloodstream form
cAMP	cyclic AMP
DHFR	dihydrofolate reductase
γECS	γ-glutamylcysteine synthetase
HTS	high-throughput screening
HAT	Human African Trypanosomiasis
MoA	mechanism-of-action
MTX	methotrexate
MD	molecular dynamics
DHCH	N^5,N^{10}-methylenetetrahydrofolate dehydrogenase/cyclohydrolase
PDE	phosphodiesterase
PTR1	pteridine reductase 1
RD-4D-QSAR	receptor-dependent four-dimensional quantitative structure-activity relationship
SAR	structure-activity-relationship
SBDD	structure-based drug design
*Tb*PTR1	*Trypanosoma brucei* pteridine reductase 1
TrypR	trypanothione reductase
TrypS	trypanothione synthetase
VS	virtual screening

References

Amata, E., N.D. Bland, C.T. Hoyt, L. Settimo, R.K. Campbell and M.P. Pollastri. 2014. Repurposing human PDE4 inhibitors for neglected tropical diseases: design, synthesis and evaluation of cilomilast analogues as Trypanosoma brucei PDEB1 inhibitors. Bioorg. Med. Chem. Lett. 24: 4084–4089.

Ancizu, S., E. Moreno, E. Torres, A. Burguete, S. Pérez-Silanes, D. Benítez et al. 2009. Heterocyclic-2-carboxylic acid (3-Cyano-1,4-di-N-oxidequinoxalin-2-yl)amide derivatives as hits for the development of neglected disease drugs. Molecules. 14: 2256–2272.

Andriani, G., E. Amata, J. Beatty, Z. Clements, B.J. Coffey, G. Courtemanche et al. 2013. Antitrypanosomal lead discovery: identification of a ligand-efficient inhibitor of Trypanosoma cruzi CYP51 and parasite growth. J. Med. Chem. 56(6): 2556–2567.

Arafet, K., S. Ferrer and V. Moliner. 2015. First quantum mechanics/molecular mechanics studies of the inhibition mechanism of cruzain by peptidyl halomethyl ketones. Biochemistry. 54: 3381–3391.

Arafet, K., S. Ferrer, F.V. González and V. Moliner. 2017. Quantum mechanics/molecular mechanics studies of the mechanism of cysteine protease inhibition by peptidyl-2,3-epoxyketones. Phys. Chem. Chem. Phys. 19: 12740–12748.

Argüelles, A.J., G.A. Cordell and H. Maruenda. 2016. Molecular docking and binding mode analysis of plant alkaloids as *in vitro* and *in silico* inhibitors of trypanothione reductase from *Trypanosoma cruzi*. Nat. Prod. Commun. 11: 57–62.

Arias, D.G., F.E. Herrera, A.S. Garay, D. Rodrigues, P.S. Forastieri, L.E. Luna et al. 2017. Rational design of nitrofuran derivatives: Synthesis and valuation as inhibitors of *Trypanosoma cruzi* trypanothione reductase. Eur. J. Med. Chem. 25: 1088–1097.

Avelar, L.A.A., C.D. Camilo, S. de Albuquerde, W.B. Fernandes, C. Gonçalez, P.W. Kenny et al. 2015. Molecular design, synthesis and trypanocidal activity of dipeptidyl nitriles as cruzain inhibitors. PLoS Negl. Trop. Dis. 9: e0003916.

Bello, A.R., B. Nare, D. Freedman, L. Hardy and S.M. Beverley. 1994. PTR1: A reductase mediating salvage of oxidized pteridines and methotrexate resistance in the protozoan parasite Leishmania major. Proc. Natl. Acad. Sci. USA. 91: 11442–11446.

Benítez, D., A. Medeiros, L. Fiestas, E.A. Panozzo-Zenere, F. Maiwald, K.C. Prousis et al. 2016. Identification of novel chemical scaffolds inhibiting trypanothione synthetase from pathogenic trypanosomatids. PLoS Negl. Trop. Dis. 10: e0004617.

Bern, C., S. Kjos, M.J. Yabsley and S.P. Montgomery. 20101 Trypanosoma cruzi and Chagas' disease in the United States. Clin. Microbiol. Rev. 24(4): 655–81.

Bettiol, E., M. Samanovic, A.S. Murkin, J. Raper, F. Buckner and A. Rodriguez. 2009. Identification of three classes of heteroaromatic compounds with activity against intracellular Trypanosoma cruzi by chemical library screening. PLoS Neglected Trop. Dis. 3: e384.

Bhambra, A.S., M. Edgar, M.R.J. Elsegood, Y. Li, G.W. Weaver, R.R.J. Arroo et al. 2016. Design, synthesis and antitrypanosomal activities of 2,6-disubstituted-4,5,7-trifluorobenzothiophenes. Eur. J. Med. Chem. 108: 347–353.

Bhambra, A.S., K.C. Ruparelia, H.L. Tan, D. Tasdemir, H. Burrell-Saward, V. Yardley et al. 2017. Synthesis and antitrypanosomal activities of novel pyridylchalcones. Eur. J. Med. Chem. 128: 213–218.

Blaazer, A.R., A.K. Singh, E. de Heuvel, E. Edink, K.M. Orrling, J.J.N. Veerman et al. 2018. Targeting a subpocket in *Trypanosoma brucei* phosphodiesterase B1 (*Tbr*PDEB1) enables the structure-based discovery of selective inhibitors with trypanocidal activity. J. Med. Chem. 61: 3870–3888.

Borsari, C., R. Luciani, C. Pozzi, I. Poehner, S. Henrich, M. Trande et al. 2016. Profiling of flavonol derivatives for the development of antitrypanosomatidic drugs. J. Med. Chem. 59: 7598–7616.

Buckner, F.S. and J.A. Urbina. 2012. Recent developments in sterol 14-demethylase inhibitors for chagas disease. Int. J. Parasitol. Drugs. Drug. Resist. 2: 236–242.

Buchynskyy, A., J.R. Gillespie, Z.M. Herbst, R.M. Ranade, F.S. Buckner and M.H. Gelb. 2017a. 1-Benzyl-3-aryl-2-thiohydantoin derivatives as new anti-Trypanosoma brucei agents: SAR and in-vivo efficacy. ACS Med. Chem. Lett. 8: 886–891.

Buchynskyy, A., J.R. Gillespie, M.A. Hulverson, J. McQueen, S.A. Creason, R.M. Ranade et al. 2017b. Discovery of N-(2-aminoethyl)-N-benzyloxyphenyl benzamides: New potent *Trypanosoma brucei* inhibitors. Bioorg. Med. Chem. 25: 1571–1584.

Büscher, P., G. Cecchi, V. Jamonneau and G. Priotto. 2017. Human African trypanosomiasis. Lancet. 390: 2397–2409.

Calvet, C.M., D.F. Viera, J.Y. Choi, D. Kellar, M.D. Cameron, J.L. Siqueira-Neto et al. 2014. 4-Aminopyridyl-based CYP51 inhibitors as anti-*Trypanosoma cruzi* drug leads with improved pharmacokinetic profile and *in vivo* potency. J. Med. Chem. 57(16): 6989–7005.

Caminos, A.P., E.A. Panozzo-Zenere, S.R. Wilkinson, B.L. Tekwani and G.R. Labadie. 2012. Synthesis and antikinetoplastid activity of a series of N,N'-substituted diamines. Bioorg. Med. Chem. Lett. 22: 1712–1715.

Cardoso, M.V.O., L.R.P. Siqueira, E.B. Silva, L.B. Costa, M.Z. Hernandes, M.M. Rabello et al. 2014. 2-Pyridyl thiazoles as novel anti-*Trypanosoma cruzi* agents: Structural design, synthesis and pharmacological evaluation. Eur. J. Med. Chem. 86: 48–59.

Carneiro, P.F., S.B. do Nascimento, A.V. Pinto, M. do Carmo, F.R. Pinto, G.C. Lechuga et al. 2012. New oxirane derivatives of 1,4-naphthoquinones and their evaluation against *T. cruzi* epimastigote forms. Bioorg. Med. Chem. 20: 4995–5000.

Cavazzuti, A., G. Paglietti, W.N. Hunter, F. Gamarro, S. Piras, M. Loriga et al. 2008. Proc. Natl. Acad. Sci. USA. 105(5): 1448–1453.

Chacón-Vargas, K.F., B. Nogueda-Torres, L.E. Sánchez-Torres, E. Suarez-Contreras, J.C. Villalobos-Rocha, Y. Torres-Martinez et al. 2017. Trypanocidal activity of quinoxaline 1,4 Di-N-oxide derivatives as trypanothione reductase inhibitors. Molecules. 22: E220.

Chappuis, F., N. Udayraj, K. Stietenroth, A. Meussen and P.A. Bovier. 2005. Eflornithine is safer than melarsoprol for the treatment of second-stage *Trypanosoma brucei* gambiense human African trypanosomiasis. Clin. Infect. Dis. 41: 748–51.

Chatelain, E. and J.-R. Ioset. 2011. Drug discovery and development for neglected diseases: the DNDi model. Drug Des. Devel. Ther. Dove Medical Press. 5: 175–181.

Chen, C.-K., S.S.F. Leung, C. Guilbert, M.P. Jacobson, J.H. McKerrow and L.M. Podust. 2010. Structural characterization of CYP51 from *Trypanosoma cruzi* and *Trypanosoma brucei* bound to the antifungal drugs posaconazole and fluconazole. PLoS Negl. Trop. Dis. 4(4): e651.

Choi, J.Y., C.M. Calvet, S.S. Gunatilleke, C. Ruiz, M.D. Cameron, J.H. McKerrow et al. 2013. Rational development of 4-aminopyridyl-based inhibitors targeting *Trypanosoma cruzi* CYP51 as anti-chagas agents. J. Med. Chem. 56(19): 7651–7668.

Cianni, L., G. Sartori, F. Rosini, D. De Vita, G. Pires, B.R. Lopes et al. 2018. Leveraging the cruzain S3 subsite to increase affinity for reversible covalent inhibitors. Bioorg. Chem. 79: 285–292.

Cleghorn, L.A.T., S. Albrecht, L. Stojanovski, F.R.J. Simeons, S. Norval, R. Kime et al. 2015. Discovery of indoline-2-carboxamide derivatives as a new class of brain-penetrant inhibitors of *Trypanosoma brucei*. J. Med. Chem. 58: 7695–7706.

Cullen, D.R. and M. Mocerino. 2017. A brief review of drug discovery research for human African trypanosomiasis. Curr. Med. Chem. 24(7): 701–17.

Cullia, G., L. Tamborini, P. Conti, C. De Micheli and A. Pinto. 2018. Folates in *Trypanosoma brucei*: Achievements and opportunities. ChemMedChem: Epub ahead of print.

da Rocha Pita, S.S., M.G.A. Albuquerque, C.R. Rodrigues, H.C. Castro and A.J. Hopfinger. 2012. Receptor-dependent 4D-QSAR analysis of peptidemimetic inhibitors of *Trypanosoma cruzi* trypanothione reductase with receptor-based alignment. Chem. Biol. Drug. Des. 79: 740–748.

Dawson, A., F. Gibellini, N. Sienkiewicz, L.B. Tulloch, P.K. Fyfe, K. McLuskey et al. 2006. Structure and reactivity of *Trypanosoma brucei* pteridine reductase: inhibition by the archetypal antifolate methotrexate. Mol. Microbiol. 61(6): 1457–1468.

De Gasparo, R., E. Brodbeck-Persch, S. Bryson, N.B. Hentzen, M. Kaiser, E.F. Pai et al. 2018. Biological evaluation and X-ray co-crystal structures of Cyclohexylpyrrolidine ligands for trypanothione reductase, an enzyme from the redox metabolism of trypanosoma. ChemMedChem. 3: 957–967.

de Souza, A.S., M.T. de Oliveira and A.D. Andricopulo. 2017. Development of a pharmacophore for cruzain using oxadiazoles as virtual molecular probes: quantitative structure-activity relationship studies. J. Comput. Aided Mol. Des. 31: 801–816.

De Vita, D., F. Moraca, C. Zamperini, F. Pandolfi, R. Di Santo, A. Matheeussen et al. 2016. *In vitro* screening of 2-(1H-imidazol-1-yl)-1-phenylethanol derivatives as antiprotozoal agents and docking studies on *Trypanosoma cruzi* CYP51. Eur. J. Med. Chem. 113: 28–33.

Denning, D.W. and M.J. Bromley. 2015. Infectious disease. How to bolster the antifungal pipeline. Science. 347(6229): 1414–1416.

Devine, W., J.L. Woodring, U. Swaminathan, E. Amata, G. Patel, J. Erath et al. 2015. Protozoan parasite growth inhibitors discovered by cross-screening yield potent scaffolds for lead discovery. J. Med. Chem. 58: 5522–5537.

Di Pisa, F., G. Landi, L. Dello Iacono, C. Pozzi, C. Borsari, S. Ferrari et al. 2017. Chroman-4-One derivatives targeting pteridine reductase 1 and showing anti-parasitic activity. Molecules. 22(3): 426.

Doerig, C. 2004. Protein kinases as targets for anti-parasitic chemotherapy. Biochim. Biophys. Acta: Proteins Proteomics. 1697: 155−168.

Dube, D., S. Sharma, T.P. Singh and P. Kaur. 2014. Pharmacophore mapping, *In Silico* screening and molecular docking to identify selective *Trypanosoma brucei* pteridine reductase inhibitors. Mol. Inform. 33(2): 124–134.

Durrant, J.D., H. Keränen, B.A. Wilson and J.A. McCammon. 2010. Computational identification of uncharacterized cruzain binding sites. PLoS Negl. Trop. Dis. 4: e676.

Eadsforth, T.C., A. Pinto, R. Luciani, L. Tamborini, G. Cullia, C. De Micheli et al. 2015. Characterization of 2,4-Diamino-6-oxo-1,6-dihydropyrimidin-5-yl Ureido based inhibitors of *Trypanosoma brucei* fold and testing for antiparasitic activity. J. Med. Chem. 58: 7938–7948.

Ehmke, V., E. Winkler, D.W. Banner, W. Haap, W.B. Schweizer, M. Rottmann et al. 2013. Optimization of triazine nitriles as rhodesain inhibitors: structure-activity relationships, bioisosteric imidazopyridine nitriles, and X-ray crystal structure analysis with human cathepsin L. ChemMedChem. 8: 967–975.

Elizondo-Jimenez, S., A. Moreno-Herrera, R. Reyes-Olivares, E. Dorantes-Gonzalez, B. Nogueda-Torres, E.A.G. de Oliveira et al. 2017. Synthesis, biological evaluation and molecular docking of new benzenesulfonylhydrazone as potential anti-*trypanosoma cruzi* agents. Med. Chem. 13: 149–158.

Eperon, G., M. Balasegaram, J. Potet, C. Mowbray, O. Valverde and F. Chappuis. 2014. Treatment options for second-stage gambiense human African trypanosomiasis. Expert. Rev. Anti. Infect. Ther. England. 12: 1407–1417.

Faerman, C.H., S.N. Savvides, C. Strickland, M.A. Breidenbach, J.A. Ponasik, B. Ganem et al. 1996. Charge is the major discriminating factor for glutathione reductase versus trypanothione reductase inhibitors. Bioorg. Med. Chem. 4: 1247–1253.

Fairlamb, A.H. and A. Cerami. 1992. Metabolism and functions of trypanothione in the Kinetoplastida. Annu. Rev. Microbiol. 46: 695–729.

Fairlamb, A.H. and D. Horn. 2018. Melarsoprol resistance in African trypanosomiasis. Trends Parasitol. 34: 481–492.

Feasey, N., M. Wansbrough-Jones, D.C.W. Mabey and A.W. Solomon. 2010. Neglected tropical diseases. Br. Med. Bull. England. 93: 179–200.

Ferrari, S., F. Morandi, D. Motiejunas, E. Nerini, S. Henrich, R. Luciani et al. 2011. Virtual screening identification of nonfolate compounds, including a CNS drug, as antiparasitic agents inhibiting pteridine reductase. J. Med. Chem. 54: 211–221.

Ferreira, L.G. and A.D. Andricopulo. 2017. Targeting cysteine proteases in trypanosomatid disease drug discovery. Pharmacol. Ther. 180: 49–61.

Ferreira, R.S., A. Simeonov, A. Jadhav, O. Eidam, B.T. Mott, M.J. Keiser et al. 2010. Complementarity between a docking and a high-throughput screen in discovering new cruzain inhibitors. J. Med. Chem. 53: 4891–4905.

Ferreira de Almeida Fuiza, L., R.B. Peres, M.R. Simões-Silva, P.B. da Silva, D. da Gama Jaen Batista, C. da Silva et al. 2018. Identification of Pyrazolo[3,4-e][1,4]thiazepin based CYP51 inhibitors as potential Chagas disease therapeutic alternative: *In vitro* and *in vivo* evaluation, binding mode prediction and SAR exploration. Eur. J. Med. Chem. 149: 257–268.

Ferrins, L., M. Gazdik, R. Rahmani, S. Varghese, M.L. Sykes, A.J. Jones et al. 2014. Pyridyl benzamides as a novel class of potent inhibitors for the kinetoplastid *Trypanosoma brucei*. J. Med. Chem. 57: 6393–6402.

Filardy, A.A., K. Guimaraes-Pinto, M.P. Nunes, K. Zukeram, L. Fliess L. Pereira et al. 2018. Human kinetoplastid protozoan infections: Where Are We Going Next? Front Immunol. Switzerland. 9: 1493.

Filho, G.B.O., M.V.O. Cardoso, J.W.P. Espíndola, D.A.O. Silva, R.S. Ferreira, P.L. Coelho et al. 2017. Structural design, synthesis and pharmacological evaluation of thiazoles against *Trypanosoma cruzi*. Eur. J. Med. Chem. 141: 346–361.

Frearson, J.A., P.G. Wyatt, I.H. Gilbert and A.H. Fairlamb. 2007. Target assessment for antiparasitic drug discovery. Trends Parasitol. 23: 589−595.

Friggeri, L., L. Scipione, R. Costi, M. Kaiser, F. Moraca, C. Zamperini et al. 2013. New promising compounds with *in vitro* nanomolar activity against *Trypanosoma cruzi*. ACS Med. Chem. Lett. 4(6): 538–541.

Friggeri, L., T.Y. Hargrove, G. Rachakonda, A.D. Williams, Z. Wawrzak, R. Di Santo et al. 2014. Structural basis for rational design of inhibitors targeting *Trypanosoma cruzi* sterol 14α-demethylase: two regions of the enzyme molecule potentiate its inhibition. J. Med. Chem. 57(15): 6704–6717.

Fytas, C., G. Zoidis, N. Tzoutzas, M.C. Taylor, G. Fytas and J.M. Kelly. 2011. Novel lipophilic acetohydroxamic acid derivatives based on conformationally constrained spiro carbocyclic 2,6-diketopiperazine scaffolds with potent trypanocidal activity. J. Med. Chem. 54: 5250–5254.

Gilbert, I.H. 2013. Drug discovery for neglected diseases: molecular target-based and phenotypic approaches: Miniperspectives series on phenotypic screening for antiinfective targets. J. Med. Chem. American Chemical Society. 56: 7719–7726.

Giordani, F., L.J. Morrison, T.G. Rowan, H.P. De Koning and M.P. Barrett. 2016. The animal trypanosomiasis and their chemotherapy: a review. Parasitology. 143: 1862–1889.

Giroud, M., U. Dietzel, L. Anselm, D. Banner, A. Kuglstatter, J. Benz et al. 2018. Repurposing a library of human cathepsin L ligands: Identification of macrocyclic lactams as potent rhodesain and *Trypanosoma brucei* inhibitors. J. Med. Chem. 61: 3350–3369.

González-Chávez, Z., V. Olin-Sandoval, J.S. Rodíguez-Zavala, R. Moreno-Sánchez and E. Saavedra. 2015. Metabolic control analysis of the *Trypanosoma cruzi* peroxide detoxification pathway identifies tryparedoxin as a suitable drug target. Biochim. Biophys. Acta. 1850: 263–273.

Guedes, P.M.M., G.K Silva, F.R.S. Gutierrez and J.S. Silva. 2011. Current status of Chagas disease chemotherapy. Expert. Rev. Anti Infect. Ther. 9: 609–620.

Gunatilleke, S.S., C.M. Calvet, J.B. Johnston, C.-K. Chen, G. Erenburg, J. Gut et al. 2012. Diverse inhibitor chemotypes targeting *Trypanosoma cruzi* CYP51. PLoS Negl. Trop. Dis. 6(7): e1736.

Haasen, D., U. Schopfer, C. Antczak, C. Guy, F. Fuchs and P. Selzer. 2017. How phenotypic screening influenced drug discovery: Lessons from five years of practice. Assay Drug Dev Technol. United States. 15: 239–246.

Hargrove, T.Y., Z. Wawrzak, P.W. Alexander, J.H. Chaplin, M. Keenan, S.A. Charman et al. 2013. Complexes of *Trypanosoma cruzi* sterol 14α-demethylase (CYP51) with two pyridine-based drug candidates for Chagas disease: structural basis for pathogen selectivity. J. Biol. Chem. 288(44): 31602–31615.

Hartmann, A.P., M.R. de Carvalho, L.S.C. Bernandes, M.H. de Moraes, E.B. de Melo, C.D. Lopes et al. 2017. Synthesis and 2D-QSAR studies of neolignan-based diaryl-tetrahydrofuran and -furan analogues with remarkable activity against *Trypanosoma cruzi* and assessment of the trypanothione reductase activity. Eur. J. Med. Chem. 140: 187–199.

Hawser, S., S. Lociuro and K. Islam. 2006. Dihydrofolate reductase inhibitors as antibacterial agents. Biochem. Pharmacol. 71(7): 941–948.

Hiltensperger, G., N.G. Jones, S. Niedermeier, A. Stich, M. Kaiser, J. Jung et al. 2012. Synthesis and structure-activity relationships of new quinolone-type molecules against *Trypanosoma brucei*. J. Med. Chem. 55: 2538–2548.

Hoekstra, W. J., T.Y. Hargrove, Z. Wawrzak, D. da Gama Jaen Batista, C.F. da Silva, A.S.G. Nefertiti et al. 2015. Clinical candidate VT-1161's antiparasitic effect *in vitro*, activity in a murine model of chagas disease, and structural characterization in complex with the target enzyme CYP51 from *Trypanosoma cruzi*. Antimicrob. Agents Chemother. 60(2): 1058–1066.

Hoelz, L.V.B., V.F. Leal, C.R. Rodrigues, P.G. Pascutti, M.G. Albuquerque, E.M.F. Muri et al. 2016. Molecular dynamics simulations of the free and inhibitor-bound cruzain systems in aqueous solvent: insights on the inhibition mechanism in acidic pH. J. Biomol. Struct. Dyn. 34: 1969–1978.

Hwang, J.Y., D. Smithson, M. Connelly, J. Maier, F. Zhu and K.R. Guy. 2010. Discovery of halo-nitrobenzamides with potential application against human African trypanosomiasis. Bioorg. Med. Chem. Lett. 20: 149–152.

Hwang, J.Y., D. Smithson, F. Zhu, G. Holbrook, M.C. Connelly, M. Kaiser et al. 2013a. Optimization of Chloronitrobenzamides (CNBs) as therapeutic leads for Human African Trypanosomiasis (HAT). J. Med. Chem. 56: 2850–2860.

Hwang, J.Y., D.C. Smithson, G. Holbrook, F. Zhu, M.C. Connelly, M. Kaiser et al. 2013b. Optimization of the electrophile of chloronitrobenzamide leads active against *Trypanosoma brucei*. Bioorg. Med. Chem. Lett. 23: 4127–4131.

Jacobs, R.T., B. Nare, S.A. Wring, M.D. Orr, D. Chen, J.M. Sligar et al. 2011. SCYX-7158, an orally-active benzoxaborole for the treatment of stage 2 human African trypanosomiasis. PLoS Negl. Trop. Dis. 5(6): e1151.

Jansen, C., H. Wang, A.J. Kooistra, C. de Graaf, K. Orrling, H. Tenor et al. 2013. Discovery of novel *Trypanosoma brucei* phosphodiesterase B1 inhibitors by virtual screening against the unliganded *Tbr*PDEB1 crystal structure. J. Med. Chem. 56: 2087–2096.

Jedwabny, W., J. Panecka-Hofman, E. Dyguda-Kazimierowicz, R.C. Wade, W.A. Sokalski. 2017. J. Comput. Aided Mol. Des. 31(8): 715–728.

Jones, B.D., A. Tochowicz, Y. Tang, M.D. Cameron, L.-I. McCall, K. Hirata et al. 2015. Synthesis and evaluation of oxyguanidine analogues of the cysteine protease inhibitor WRR-483 against Cruzain. ACS Med. Chem. Lett. 7: 77–82.

Jones, A.J. and V.M. Avery. 2015. Future treatment options for human African trypanosomiasis. Expert Rev. Anti Infect. Ther. 13: 1429–1432.

Kelly, J.M., M.C. Taylor, D. Horn, E. Loza, I. Kalvinsh and F. Björkling. 2012. Inhibitors of human histone deacetylase with potent activity against the African trypanosome *Trypanosoma brucei*. Bioorg. Med. Chem. Lett. 22: 1886–1890.

Kennedy, P.G.E. 2013. Clinical features, diagnosis, and treatment of human African trypanosomiasis (sleeping sickness). Lancet Neurol. Elsevier Ltd. 12: 186–194.

Khalaf, A.I., J.K. Huggan, C.J. Suckling, C.L. Gibson, K. Stewart, F. Giordani et al. 2014. Structure-based design and synthesis of antiparasitic pyrrolopyrimidines targeting pteridine reductase 1. J. Med. Chem. 57(15): 6479–6494.

Khraiwesh, M.H., C.M. Lee, Y. Brandy, E.S. Akinboye, S. Berhe, G. Gittens et al. 2012. Antitrypanosomal activities and cytotoxicity of some novel imidosubstituted 1,4-Naphthoquinone derivatives. Arch. Pharm. Res. 35: 27–33.

Krieger, S., W. Schwarz, M.R. Ariyanayagam, A.H. Fairlamb, R.L. Krauth-Siegel and C. Clayton. 2000. Trypanosomes lacking trypanothione reductase are avirulent and show increased sensitivity to oxidative stress. Mol. Microbiol. 35: 542–552.

Lass-Flörl, C. 2011. Triazole antifungal agents in invasive fungal infections: a comparative review. Drugs. 71(18): 2405–2419.

Lepesheva, G.I. and M.R. Waterman. 2004. CYP51—the omnipotent P450. Mol. Cell. Endocrinol. 215(1-2): 165–170.

Lepesheva, G.I. and M.R. Waterman. 2007. Sterol 14alpha-demethylase cytochrome P450 (CYP51), a P450 in all biological kingdoms. Biochim. Biophys. Acta. 1770(3): 467–477.

Lepesheva, G.I., H.-W. Park, T.Y. Hargrove, B. Vanhollebeke, Z. Wawrzak, J.M. Harp et al. 2010. Crystal structures of *Trypanosoma brucei* sterol 14alpha-demethylase and implications for selective treatment of human infections. J. Biol. Chem. 285: 1773–1780.

Lepesheva, G.I., T.Y. Hargrove, G. Rachakonda, Z. Wawrzak, S. Pomel, S. Cojean et al. 2015. VFV as a new effective CYP51 structure-derived drug candidate for chagas disease and visceral leishmaniasis. J. Infect. Dis. 212(9): 1439–1448.

Lepesheva, G.I., L. Friggeri and M.R. Waterman. 2018. CYP51 as drug targets for fungi and protozoan parasites: past, present and future. Parasitology. 1–17.

Leroux, A.E. and R.L. Krauth-Siegel. 2016. Thiol redox biology of trypanosomatids and potential targets for chemotherapy. Mol. Biochem. Parasitol. 206: 67–74.

Liese, B., M. Rosenberg and A. Schratz. 2010. Programmes, partnerships, and governance for elimination and control of neglected tropical diseases. Lancet. 375: 67–76.

Linciano, P., A. Dawson, I. Pöhner, D.M. Costa, M.S. Sá, A. Cordeiro-da-Silva et al. 2017. Exploiting the 2□Amino-1,3,4-thiadiazole scaffold to inhibit *Trypanosoma brucei* pteridine reductase in support of early-stage drug discovery. ACS Omega. 2: 5666–5683.

Martins, L.C., P.H.M. Torres, R.B. de Oliveira, P.G. Pascutti, E.A. Cino, R.S. Ferreira. 2018. Investigation of the binding mode of a novel cruzain inhibitor by docking, molecular dynamics, ab initio and MM/PBSA calculations. J. Comput. Aided Mol. Des. 32: 591–605.

Mendoza-Martínez, C., J. Correa-Basurto, R. Nieto-Meneses, A. Márquez-Navarro, R. Aguilar-Suárez, M.D. Montero-Cortes et al. 2015. Design, synthesis and biological evaluation of quinazoline derivatives as anti-trypanosomatid and anti-plasmodial agents. Eur. J. Med. Chem. 96: 296–307.

Mesu, V.K.B.K., W.M. Kalonji, C. Bardonneau, O.V. Mordt, S. Blesson, F. Simon et al. 2018. Oral fexinidazole for late-stage African *Trypanosoma brucei* gambiense trypanosomiasis: a pivotal multicentre, randomised, non-inferiority trial. Lancet. 391(10116): 144–54.

MMV Medicines for Malaria Venture. 2018. Developing antimalarials to save lives. https://www.mmv.org/.

Montalvo-Quirós, S., A. Taladriz-Sender, M. Kaiser and C. Dardonville. 2015. Antiprotozoal activity and DNA binding of dicationic acridones. J. Med. Chem. 58: 1940–1949.

Mpamhanga, C.P., D. Spinks, L.B. Tulloch, E.J. Shanks, D.A. Robinson, I.T. Collie et al. 2009. One scaffold, three binding modes: Novel and selective pteridine reductase 1 inhibitors derived from fragment hits discovered by virtual screening. J. Med. Chem. 52(14): 4454–4465.

Muscia, G.C., S.I. Cazorla, F.M. Frank, G.L. Borosky, G.Y. Buldain, S.E. Asís et al. 2011. Synthesis, trypanocidal activity and molecular modeling studies of 2-alkylaminomethylquinoline derivatives. Eur. J. Med. Chem. 46: 3696–3703.

Njiokou, F., H. Nimpaye, G. Simo et al. 2010. Domestic animals as potential reservoir hosts of *Trypanosoma brucei* gambiense in sleeping sickness foci in Cameroon. Parasite. 17: 61–66.

Ochiana, S.O., A. Gustafson, N. Bland, C. Wang, M.J. Russo, R.K. Campbell et al. 2012. Synthesis and evaluation of human phosphodiesterases (PDE) 5 inhibitor analogs as trypanosomal PDE inhibitors. Part 2. Tadalafil analogs. Bioorg. Med. Chem. Lett. 22: 2582–2584.

Olin-Sandoval, V., Z. González-Chávez, M. Berzunza-Cruz, I. Martínez, R. Jasso-Chávez, I. Becker et al. 2012. Drug target validation of the trypanothione pathway enzymes through metabolic modelling. FEBS J. 279: 1811–1833.

Okello, A.L., K. Bardosh, J. Smith and S.C. Welburn. 2014. One health: Past successes and future challenges in three African contexts. PLoS Negl. Trop. Dis. 8: 1–7.

Ong, H.B., N. Sienkiewicz, S. Wyllie and A.H. Fairlamb. 2011. Dissecting the metabolic roles of pteridine reductase 1 in *Trypanosoma brucei* and Leishmania major. J. Biol. Chem. 286(12): 10429–10438.

Orrling, K.M., C.X.L. Jansen Jansen, V. Balmer, P. Bregy, A. Shanmugham, P. England et al. 2012. Catechol pyrazolinones as trypanocidals: fragment-based design, synthesis, and pharmacological evaluation of nanomolar inhibitors of trypanosomal phosphodiesterase B1. J. Med. Chem. 55: 8745–8756.

Palos, I., E.E. Lara-Ramirez, J.C. Lopez-Cedillo, C. Garcia-Perez, M. Kashif, V. Bocanegra-Garcia et al. 2017. Repositioning FDA drugs as potential cruzain inhibitors from *Trypanosoma cruzi*: Virtual screening, *in vitro and in vivo* studies. Molecules. 22: E1015.

Pan, D., Y. Tseng and A.J. Hopfinger. 2003. Quantitative structure-based design: formalism and application of receptor-dependent RD-4D-QSAR analysis to a set of glucose analogue inhibitors of glycogen phosphorylase. J. Chem. Inf. Comput. Sci. 43: 1591–1607.

Panecka-Hofman, J., I. Pöhner, F. Spyrakis, T. Zeppelin, F. Di Pisa, L. Dello Iacono et al. 2017. Comparative mapping of on-targets and off-targets for the discovery of anti-trypanosomatid folate pathway inhibitors. Biochim. Biophys. Acta. 1861: 3215–3230.

Papadopoulou, M.V., W.D. Bloomer, H.S. Rosenzweig and M. Kaiser. 2017. The antitrypanosomal and antitubercular activity of some nitro(triazole/imidazole)-based aromatic amines. Eur. J. Med. Chem. 138: 1106–1113.

Patel, G., C.E. Karver, R. Behera, P.J. Guyett, C. Sullenberger, P. Edwards et al. 2013. Kinase scaffold repurposing for neglected disease drug discovery: Discovery of an efficacious, Lapatanib-derived lead compound for trypanosomiasis. J. Med. Chem. 56: 3820–3832.

Patrick, D.A., T. Wenzler, S. Yang, P.T. Weiser, M.Z. Wang, R. Brun et al. 2016. Synthesis of novel amide and urea derivatives of thiazol-2-ethylamines and their activity against Trypanosoma brucei rhodesiense. Bioorg. Med. Chem. 24: 2451–2465.

Patrick, D.A., J.R. Gillespie, J. McQueen, M.A. Hulverson, R.M. Ranade, S.A. Creason et al. 2017. Urea derivatives of 2-aryl-benzothiazol-5-amines: A new class of potential drugs for human African trypanosomiasis. J. Med. Chem. 60: 957–971.

Patterson, S., M.S. Alphey, D.C. Jones, E.J. Shanks, I.P. Street, J.A. Frearson et al. 2011. Dihydroquinazolines as a novel class of *Trypanosoma brucei* trypanothione reductase inhibitors: Discovery, synthesis, and characterization of their binding mode by protein crystallography. J. Med. Chem. 54: 6514–6530.

Pauli, I., L.G. Ferreira, M.L. de Souza, G. Oliva, R.S. Ferreira, M.A. Dessoy et al. 2017. Molecular modeling and structure-activity relationships for a series of benzimidazole derivatives as cruzain inhibitors. Future Med. Chem. 9: 641–657.

Pérez-Molina, J.A. and I. Molina. 2018. Chagas disease. Lancet. 391: 82–94.

Persch, E., S. Bryson, N.K. Todoroff, C. Eberle, J. Thelemann, N. Dirdjaja et al. 2014. Binding to large enzyme pockets: small-molecule inhibitors of trypanothione reductase. ChemMedChem. 9: 1880–1891.

Pierce, R.J., J. MacDougall, R. Leurs and M.P. Costi. 2017. The future of drug development for neglected tropical diseases: How the european commission can continue to make a difference. Trends Parasitol. Elsevier Ltd. 33: 581–583.

Price, H.P., M.R. Menon, C. Panethymitaki, D. Goulding, P.G. McKean and D.F. Smith. 2003. Myristoyl-CoA:protein N-myristoyl-transferase, an essential enzyme and potential drug target in kinetoplastid parasites. J. Biol. Chem. 278: 7206−7214.

Priotto, G., S. Kasparian, W. Mutombo, D. Ngouama, S. Ghorashian, U. Arnold et al. 2009. Nifurtimox-eflornithine combination therapy for second-stage African *Trypanosoma brucei* gambiense trypanosomiasis: a multicentre, randomised, phase III, non-inferiority trial. Lancet (London, England). England. 374: 56–64.

Rahmani, R., K. Ban, A.J. Jones, L. Ferrins, D. Ganame, M.L. Sykes et al. 2015. 6-Arylpyrazine-2-carboxamides: A new core for *Trypanosoma brucei* inhibitors. J. Med. Chem. 58: 6753–6765.

Reid, C.S., D.A. Patrick, S. He, J. Fotie, K. Premalatha, R.R. Tidwell et al. 2011. Synthesis and antitrypanosomal evaluation of derivatives of N-benzyl-1,2-dihydroquinolin-6-ols: Effect of core substitutions and salt formation. Bioorg. Med. Chem. 19: 513–523.

Rodriques Coura, J. and S.L. de Castro. 2002. A critical review on Chagas disease chemotherapy. Mem. Inst. Oswaldo Cruz. Brazil. 97: 3–24.

Rodrigues, R.F., D. Castro-Pinto, A. Echevarria, C.M. dos Reis, C.N. Del Cistia, C.M. Sant'Anna et al. 2012. Investigation of trypanothione reductase inhibitory activity by 1,3,4-thiadiazolium-2-aminide derivatives and molecular docking studies. Bioorg. Med. Chem. 20: 1760–1766.

Russell, S., R. Rahmani, A.J. Jones, H.L. Newson, K. Neilde, I. Cotillo et al. 2016. Hit-to-lead optimization of a novel class of potent, broad-spectrum trypanosomacides. J. Med. Chem. 59: 9686–9720.

Samant, B.S. and C. Chakaingesu. 2013. Novel naphthoquinone derivatives: Synthesis and activity against human African trypanosomiasis. Bioorg. Med. Chem. Lett. 23: 1420–1423.

Sánchez-Moreno, M., C. Marín, P. Navarro, L. Lamarque, E. García-España, C. Miranda et al. 2012. *In vitro* and *in vivo* trypanosomicidal activity of pyrazole-containing macrocyclic and macrobicyclic polyamines: Their action on acute and chronic phases of Chagas disease. J. Med. Chem. 55: 4231–4243.

Sands, M., M.A. Kron and R.B. Brown. 1985. Pentamidine: a review. Rev Infect Dis. United States. 7: 625–63.

Schirmeister, T., J. Schmitz, S. Jung, T. Schmenger, R.L. Krauth-Siegel and M. Gütschow. 2017. Evaluation of dipeptide nitriles as inhibitors of rhodesain, a major cysteine protease of *Trypanosoma brucei*. Bioorg. Med. Chem. Lett. 27: 45–50.

Schormann, N., B. Pal, O. Senkovich, M. Carson, A. Howard, C. Smith et al. 2005. Crystal structure of *Trypanosoma cruzi* pteridine reductase 2 in complex with a substrate and an inhibitor. J. Struct. Biol. 152: 64–75.

Schormann, N., O. Senkovich, K. Walker, D.L. Wright, A.C. Anderson, A. Rosowsky et al. 2008. Structure-based approach to pharmacophore identification, *in silico* screening, and three-dimensional quantitative structure-activity relationship studies for inhibitors of *Trypanosoma cruzi* dihydrofolate reductase function. Proteins. 73: 889–901.

Schormann, N., S.E. Velu, S. Murugesan, O. Senkovich, K. Walker, B.C. Chenna et al. 2010. Synthesis and characterization of potent inhibitors of *Trypanosoma cruzi* dihydrofolate reductase. Bioorg. Med. Chem. 18: 4056–4066.

Setzer, W.N. and I.V. Ogungbe. 2012. *In-silico* investigation of antitrypanosomal phytochemicals from Nigerian medicinal plants. PLoS Negl. Trop. Dis. 6(7): e1727.

Shuvalov, O., A. Petukhov, A. Daks, O. Fedorova, E. Vasileva, N.A. Barlev. 2017. One-carbon metabolism and nucleotide biosynthesis as attractive targets for anticancer therapy. Oncotarget. 8(14): 23955–23977.

Sienkiewicz, N., H.B. Ong and A.H. Fairlamb. 2010. *Trypanosoma brucei* pteridine reductase 1 is essential for survival *in vitro* and for virulence in mice. Mol. Microbiol. 77(3): 658–671.

Silva, D.G., J.R. Rocha, G.R. Sartori and C.A. Montanari. 2017. Highly predictive hologram QSAR models of nitrile-containing cruzain inhibitors. J. Biomol. Struct. Dyn. 35: 3232–3249.

Silva, E.B., D.A.O. Silva, A.R. Oliveira, C.H.S. Mendes, T.A.R. dos Santos, A.C. da Silva et al. 2017. Desing and synthesis of potent anti-*Trypanosoma cruzi* agents new thiazoles derivatives which induce apoptotic parasite death. Eur. J. Med. Chem. 130: 39–50.

Silva-Júnior, E.F., E.P.S. Silva, P.H.B. França, J.P.N. Silva, E.O. Barreto, E.B. Silva et al. 2016. Design, synthesis, molecular docking and biological evaluation of thiophen-2-iminothiazolidine derivatives for use against *Trypanosoma cruzi*. Bioorg. Med. Chem. 24: 4228–4240.

Simarro, P.P., G. Cecchi, J.R. Franco et al. 2012. Estimating and mapping the population at risk of sleeping sickness. PLoS Negl. Trop. Dis. 6: e1859

Spinks, D., H.B. Ong, C.P. Mpamhanga, E.J. Shanks, D.A. Robinson, I.T. Collie et al. 2011. Design, synthesis and biological evaluation of novel inhibitors of *Trypanosoma brucei* pteridine reductase 1. ChemMedChem. 6: 302–308.

Stank, A., D.B. Kohk, M. Horn, E. Sizikova, R. Neil, J. Panecka et al. 2017. TRAPP webserver: predicting protein binding site flexibility and detecting transient binding pockets. Nucleic Acids Res. 45: W325–W330.

Suryadevara, P.K., K.K. Racherla, S. Olepu, N.R. Norcross, H.B. Tatipaka, J.A. Arif et al. 2013. Dialkylimidazole inhibitors of Trypanosoma cruzi sterol 14α-demethylase as anti-Chagas disease agents. Bioorg. Med. Chem. Lett. 23: 6492–6499.

Tagoe, D.N.A., T.D. Kalejaiye and H.P. de Koning. 2015. The ever unfolding story of cAMP signaling in tryptrypanosoma: vive la difference! Front. Pharmacol. 6: 185.

Tapia, R.A., C.O. Salas, K. Vázquez, C. Espinosa-Bustos, J. Soto-Delgado, J. Varela et al. 2014. Synthesis and biological characterization of new aryloxyindole-4,9-diones as potent trypanosomicidal agents. Bioorg. Med. Chem. Lett. 24: 3919–3922.

Thompson, A.M., A. Blaser, B.D. Palmer, R.F. Anderson, S.S. Shinde, D. Launay et al. 2017. 6-Nitro-2,3-dihydroimidazo[2,1-b][1,3]thiazoles: Facile synthesis and comparative appraisal against tuberculosis and neglected tropical diseases. Bioorg. Med. Chem. Lett. 27: 2583–2589.

Torres, E., E. Moreno-Viguri, S. Galiano, G. Devarapally, P.W. Crawford, A. Azqueta et al. 2013. Novel quinoxaline 1,4-di-N-oxide derivatives as new potential antichagasic agents. Eur. J. Med. Chem. 66: 324–334.

Torrie, L.S., S. Wyllie, D. Spinks, S.L. Oza, S. Thompson, J.R. Harrison et al. 2009. Chemical validation of trypanothione synthetase. J. Biol. Chem. 284: 36137−36145.

Trouiller, P., E. Olliaro, J. Torreele, R. Orbinski and Laing, N. Ford. 2002. Drug development for neglected diseases: a deficient market and a public-health policy failure, Lancet (London, England). 359: 2188–94.

Tulloch, L.B., V.P. Martini, J. Iulek, J.K. Huggan, J.H. Lee, C.L. Gibson et al. 2010. Structure-based design of pteridine reductase inhibitors targeting African sleeping sickness and the leishmaniases. J. Med. Chem. 53(1): 221–229.

Upadhayaya, R.S., S.S. Dixit, A. Földesi and J. Chattopadhyaya. 2013. New antiprotozoal agents: Their synthesis and biological evaluations. Bioorg. Med. Chem. Lett. 23: 2750–2758.

Vázquez, C., M. Mejia-Tlachi, Z. González-Chávez, A. Silva, J.S. Rodríguez-Zavala, R. Moreno-Sánchez et al. 2017. Buthionine sulfoximine is a multitarget inhibitor of trypanothione synthesis in *Trypanosoma cruzi*. FEBS Lett. 591: 3881–3894.

Vázquez, K., C. Espinosa-Bustos, J. Soto-Delgado, R.A. Tapia, J. Varela, E. Birriel et al. 2015. New aryloxy-quinone derivatives as potential Anti-Chagasic agents: Synthesis, trypanosomicidal activity, electrochemical properties, pharmacophore elucidation and 3D-QSAR analysis. RSC Adv. 5: 65153–65166.

Vega, M.C., M. Rolón, A. Montero-Torres, C. Fonseca-Berzal, J.A. Escario, A. Gómez-Barrio et al. 2012. Synthesis, biological evaluation and chemometric analysis of indazole derivatives. 1,2-disubstituted 5-nitroindazolinones, new prototypes of antichagasic drug. Eur. J. Med. Chem. 58: 214–227.

Vickers, T.J. and S.M. Beverley. 2011. Folate metabolic pathways in Leishmania. Essays Biochem. 51: 63–80.

Viera, D.F., J.Y. Choi, C.M. Calvet, J.L. Siqueira-Neto, J.B. Johnston, D. Kellar et al. 2014a. Binding mode and potency of N-Indolyloxopyridinyl-4-aminopropanyl-based inhibitors targeting *Trypanosoma cruzi* CYP51. J. Med. Chem. 57(23): 10162–10175.

Viera, D.F., J.Y. Choi, W.R. Roush and L.M. Podust. 2014b. Expanding the binding envelope of CYP51 inhibitors targeting *Trypanosoma cruzi* with 4-aminopyridyl-based sulfonamide derivatives. ChemBioChem. 15(8): 1111–1120.

Villalta, F., M.C. Dobish, P.N. Nde, Y.Y. Kleshchenko, T.Y. Hargrove, C.A. Johnson et al. 2013. VNI cures acute and chronic experimental Chagas disease. J. Infect. Dis. 208(3): 504–511.

Wang, C., T.D. Ashton, A. Gustafson, N.D. Bland, S.O. Ochiana, R.K. Campbell et al. 2012. Synthesis and evaluation of human phosphodiesterases (PDE) 5 inhibitor analogs as trypanosoma PDE inhibitors. 1. Sildenafil analogs. Bioorg. Med. Chem. Lett. 22: 2579–2581.

Wermuth, C., D. Aldous, P. Raboisson and D. Rognan. 2015. The practice of medicinal chemistry. 4th edition.

WHO. 2010. Chagas disese: epidemiology. http://www.who.int/chagas/epidemiology/en/.

WHO. 2017. Human African trypanosomiasis: epidemiological situation. http://www.who.int/trypanosomiasis_african/country/en/.

Weiss, M.G. 2008. Stigma and the social burden of neglected tropical diseases. PLoS Negl. Trop. Dis. Public Library of Science. 2: e237.

Wiggers, H.J., J.R. Rocha, W.B. Fernandes, R. Sesti-Costa, Z.A. Carneiro, J. Cheleski et al. 2013. Non-peptidic cruzain inhibitors with trypanocidal activity discovered by virtual screening and *in vitro* assay. PLoS Negl. Trop. Dis. 7: e2370.

Wilcken, R., M.O. Zimmermann, A. Lange, A.C. Joerger and F.M. Boeckler. 2013. Principles and applications of halogen bonding in medicinal chemistry and chemical biology. J. Med. Chem. 56(4): 1363–1388.

Woodring, J.L., N.D. Bland, S.O. Ochiana, R.K. Campbell and M.P. Pollastri. 2013. Synthesis and assessment of catechol diether compounds as inhibitors of trypanosomal phosphodiesterase B1 (*Tbr*PDEB1). Bioorg. Med. Chem. Lett. 23: 5971–5974.

Yu, X., V. Cojocaru, G. Mustafa, O.M.H. Salo-Ahen, G.L. Lepesheva and R.C. Wade. 2015. Dynamics of CYP51: implications for function and inhibitor design. J. Mol. Recognit. 28(2): 59–73.

Yu, X., P. Nandekar, G. Mustafa, V. Cojocaru, G.L. Lepesheva and R.C. Wade. 2016. Ligand tunnels in *T. brucei* and human CYP51: Insights for parasite-specific drug design. Biochim. Biophys. Acta. 1860(1): 67–78.

Yuthavong, Y., J. Yuvaniyama, P. Chitnumsub, J. Vanichtanankul, S. Chusacultanachai, B. Tarnchompoo et al. Malarial (*Plasmodium falciparum*) dihydrofolate reductase-thymidylate synthase: structural basis for antifolate resistance and development of effective inhibitors. Parasitology. 130(3): 249–259.

Zelisko, N., D. Atamanyuk, O. Vasylenko, P. Grellier and R. Lesyk. 2012. Synthesis and antitrypanosomal activity of new 6,6,7-trisubstituted thiopyrano[2,3-d][1,3]thiazoles. Bioorg. Med. Chem. Lett. 22: 7071–7074.

Zuccotto, F., R. Brun, D. Gonzalez Pacanowska, L.M. Ruiz Perez and I.H. Gilbert. 1999. The structure-based design and synthesis of selective inhibitors of *Trypanosoma cruzi* dihydrofolate reductase. Bioorg. Med. Chem. Lett. 9: 1463–1468.